ISSN 0280–5316
ISRN LUTFD2/TFRT--5617--SE

Robust Control of a Flexible Servo with Parametric Uncertainty

Enrique Pico Marco

Department of Automatic Control
Lund Institute of Technology
May 1999

Department of Automatic Control
Lund Institute of Technology
Box 118
S-221 00 Lund Sweden

Document name
MASTER THESIS

Date of issue
May 1999

Document Number
ISRN LUTFD2/TFRT--5617--SE

Author(s)
Enrique Pico Marco

Supervisor
Anders Rantzer,
Andrey Ghulchak

Sponsoring organisation

Title and subtitle

Robust Control of a Flexible Servo with Parametric Uncertainty

Abstract

This master thesis is centered in robust control. There is a distinction between these two systems:

Robust stability The system is stable for all perturbed plants about the nominal model up to the worst-case model uncertainty.

Robust performance The system satisfies the performance specifications for all perturbed plants about the nominal model up to the worst-case model uncertainty.

Special attention is paid to the second concept. Around it, two parallel tasks have been developed. On one hand a series of control design techniques, such as mixed sensitivity and $\mathcal{H}_\infty$ loop-shaping, have been applied to an example of a flexible servo. Simulations with the nominal plant and varying certain plant parameters have been carried out in order to compare the different controllers that were obtained. Some controllers have also been applied to a real experimental setup. On the other hand two methods to represent parametric uncertainty have been analyzed, subject to a particular condition in order to be able to apply convex techniques when solving robust optimization problems.

Key words

Classification system and/or index terms (if any)

Supplementary bibliographical information

ISSN and key title
0280–5316

ISBN

Language
English

Number of pages
74

Recipient's notes

Security classification

Robust Control of a Flexible Servo with Parametric Uncertainty

Enrique Picò i Marco

May 5, 1999

Contents

List of Tables

List of Figures

Chapter 1

Introduction

Uncertainty in the plant model may have several origins: there are always parameters which are only known approximately, the parameters in the linear model may vary due to nonlinearities or changes in the operating conditions, measurement devices have imperfections ... or even when a very detailed model exists we may choose to work with a simpler nominal model.
The various sources of model uncertainty can be grouped into two main classes:

Parametric uncertainty. Here the structure of the model is known, but some of the parameters are uncertain.

Unstructured uncertainty. Here the model is in error because of missing dynamics, usually at high frequencies.

Uncertainty in the model should be taken into account not only to assure stability but also performance. In this thesis the stress is on the latter, particularly in the presence of parametric uncertainty. The flexible servo used throughout the thesis is described in Chapter 2. Chapter 3 presents a description of the uncertainty models used in the thesis. Chapter 4 contains some controller designs from a previous project. In Chapters 5 and 6 a series of controllers are developed using $\mathcal{H}_\infty$ techniques, specifically mixed sensitivity and $\mathcal{H}_\infty$ loop-shaping. Chapter 7 contains a comparison of the different designs shown up to this point. Chapter 8 presents the calculations for a particular controller design problem to which the algorithm explained in [5] can be applied. Finally Chapter 9 presents the conclusions.

Chapter 2

Process model

2.1 Description of the plant

The flexible servo used is the "Rectilinear Dynamic System.Model 210"of ECP Educational Control Products. There is a complete description in [11]. Here we give a brief summary. The mecanism consists of two mass carriages interconnected by a spring. A dashpot with adjustable damping is coupled to the second mass. Each mass carriage can load several brass weights of 500 ± 5g each, and carriage suspension is an anti-friction ball bearing type with approximately ± 3cm of available travel. Springs of various stiffness may be attached between masses. The linear drive connected to the first mass is comprised of a gear rack suspended on a carriage and pinion coupled to the brushless servo motor shaft. Optical encoders measure the mass carriage positions via a cable drive with pulley.
In order to get a linear model of the plant, it can be supposed both brushless servo and encoders only introduce constant gains. These will be taken into account in the implementation of the controllers. In practice the motor also introduces a dead zone and non-ideal effects such as motor cogging which will be neglected.
Coulomb (or static) and viscous friction between the different mechanical elements of the plant can not be neglected and will be approximately modelled as a damping of the masses with a different damping coefficient for each mass. A scheme of the model is found in figure 2.1.

Newton's second law of motion gives

$$m_1\ddot{y}_1 + c_1\dot{y}_1 + k(y_1 - y_2) = F(t)$$
$$m_2\ddot{y}_2 + c_2\dot{y}_2 + k(y_2 - y_1) = 0$$

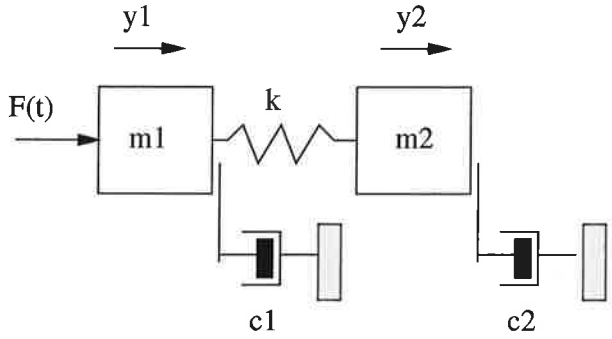

Figure 2.1: Diagram of the plant

In state space form and taking as states the positions and weighted velocities of the two masses

$$x^T = \begin{bmatrix} y_1 & \sqrt{\frac{m_1}{k}}\dot{y}_1 & y_2 & \sqrt{\frac{m_2}{k}}\dot{y}_2 \end{bmatrix}$$

gives

$$\begin{aligned} \dot{x} &= Ax + BF(t) \\ y &= Cx \end{aligned}$$

with

$$A = \begin{bmatrix} 0 & \sqrt{\frac{k}{m_1}} & 0 & 0 \\ -\sqrt{\frac{k}{m_1}} & -\frac{c_1}{m_1} & \sqrt{\frac{k}{m_1}} & 0 \\ 0 & 0 & 0 & \sqrt{\frac{k}{m_2}} \\ \sqrt{\frac{k}{m_2}} & 0 & -\sqrt{\frac{k}{m_2}} & -\frac{c_2}{m_2} \end{bmatrix}$$

$$B^T = \begin{bmatrix} 0 & \sqrt{\frac{1}{m_1 k}} & 0 & 0 \end{bmatrix}$$

$$C = \begin{bmatrix} 1 & 0 & 0 & 0 \\ 0 & 0 & 1 & 0 \end{bmatrix}$$

The state vector has been weighted, instead of taking as states the positions and velocities, in order to avoid numerical problems due to a badly

conditioned matrix A.
Since only SISO systems are going to be treated in this thesis and the goal is to control the position of the second mass, the matrix C becomes

$$C = \begin{bmatrix} 0 & 0 & 1 & 0 \end{bmatrix}$$

The transfer function from F(t) to y_2 is

$$y_2 = \frac{k}{(m_1^2 + c_1 s + k)(m_2 s^2 + c_2 s + k) - k^2} F(t)$$

For the nominal plant the medium stiffness spring and three brass weights per carriage were chosen, so it's easier to change parameter values in the real plant. These parameters have been identified as described in Appendix A and the resulting values are

k	=	423	N/m
m_1	=	2.25	Kg
m_2	=	2.07	Kg
c_1	=	3.25	Ns/m
c_2	=	8.18	Ns/m

Table 2.1: Nominal plant parameters

substituting in the transfer function and transforming to zero-pole form

$$y_2 = \frac{90.82}{s(s + 2.656)(s^2 + 2.74s + 390.8)} F(t)$$

This can be represented by

$$y_2 = \frac{Kp}{s(s + a)(s^2 + 2\zeta_p \omega_p s + \omega_p^2)} F(t)$$

with $Kp = 90.82$, $a = 2.656$, $\zeta_p = 0.069$, $\omega_p = 19.77$.

Chapter 3

Uncertainty models

There are several ways of representing uncertainty. For unstructured uncertainty the following methods are common:

1. *Direct Multiplicative perturbation.* If $G(s)$ is the nominal plant and $G_p(s)$ the perturbed one, then

$$G_p(s) = G(s)(1 + \omega_I(s)\Delta_I(s))$$

with Δ_I any stable transfer function such that $|\Delta_I(j\omega)| \leq 1 \forall \omega$ and $\omega_I(s)$ an stable weight. It is assumed that no unstable poles of $G(s)$ are canceled in forming $G_p(s)$. Thus, both have the same unstable poles. It is often used to represent uncertainty arising from high frequency unmodelled dynamics.

2. *Inverse Multiplicative perturbation.* If $G(s)$ is the nominal plant and $G_p(s)$ the perturbed one, then

$$G_p(s) = G(s)(1 + \omega_I(s)\Delta_I(s))^{-1}$$

with Δ_I any stable transfer function such that $|\Delta_I(j\omega)| \leq 1 \forall \omega$ and $\omega_I(s)$ an stable weight. Better suited for representing pole uncertainty, it allows for poles crossing the imaginary axis. On the other hand it is assumed no open loop zero crosses the imaginary axes. It is often regarded as arising from low frequency parametric uncertainty.

3. *Coprime Factor Uncertainty.*The set of perturbed plants is

$$G_p = (M_l + \Delta_M)^{-1}(N_l + \Delta_N), \quad \|[\Delta_N \ \Delta_M]\|_\infty \leq \epsilon$$

where $G = M_l^{-1}N_l$ is a left coprime factorization of the nominal plant. It can be regarded as a combination of multiplicative and inverse multiplicative uncertainty. It allows both zeros and poles to cross into the

right-half plane. In Appendix B the method to get the coprime factors of $G(s)$ is briefly outlined.

For structured uncertainty there are several methods. Of these only parametric state-space uncertainty and an extension of the coprime factor uncertainty representation, explained in [9], are going to be treated in the following sections. In the above mentioned reference uncertainty is represented by an artificial feedback loop, following the general control problem formulation represented in figure 3.1.

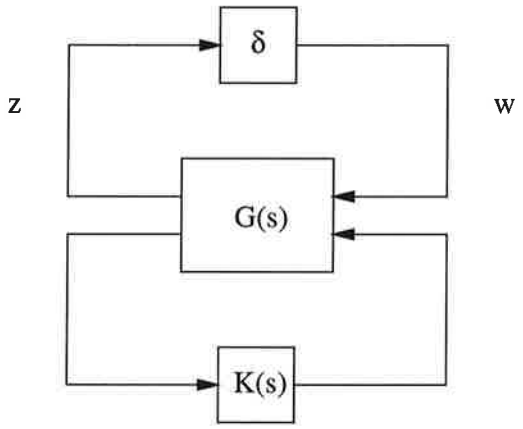

Figure 3.1: General control problem formulation

The only limitation is that w must be scalar in order to be able to apply convex optimization. The different uncertainty representations can be cast in this general setting.

3.1 Parametric state-space uncertainty

This uncertainty description has not been used in subsequent chapters, but it led to the choice of m_2 , c_2 as the only parameters to be regarded as uncertain. Consider an uncertain state-space model

$$\dot{x} = A_p x + B_p u$$
$$y = C_p x + D_p u$$

Assume the cause for uncertainty is uncertainty in some real parameters δ_1,δ_2 ... and assume for simplicity the state-space matrices depend linearly on these parameters ,

$$A_p = A + \sum \delta_i A_i, \quad B_p = B + \sum \delta_i B_i,$$

$$C_p = C + \sum \delta_i C_i, \quad D_p = D + \sum \delta_i D_i$$

where A,B,C and D model the nominal system.

The initial objective was to study the effects of uncertainty in the real parameters m_2 , c_2 , and k. It turned out it is not possible get a state-space representation in such a way that once transformed to the general setting w is scalar. The following state matrices are taken

$$A = \begin{bmatrix} 0 & 1 & 0 & 0 \\ -\frac{k}{m_1} & -\frac{c_1}{m_1} & \frac{k}{m_1} & 0 \\ 0 & 0 & 0 & 1 \\ \frac{k}{m_2} & 0 & -\frac{k}{m_2} & -\frac{c_2}{m_2} \end{bmatrix}$$

$$B^T = \begin{bmatrix} 0 & \frac{1}{m_1} & 0 & 0 \end{bmatrix}$$

$$C = \begin{bmatrix} 1 & 0 & 0 & 0 \\ 0 & 0 & 1 & 0 \end{bmatrix}$$

which have as state vector

$$x^T = \begin{bmatrix} y_1 & \dot{y}_1 & y_2 & \dot{y}_2 \end{bmatrix}$$

In this case only A is perturbed with $A_p = A + \Delta$ and

$$\Delta = \begin{bmatrix} 0 & 0 & 0 & 0 \\ \delta_1 & 0 & \delta_1 & 0 \\ 0 & 0 & 0 & 0 \\ \delta_2 & 0 & \delta_2 & \delta_3 \end{bmatrix}$$

In order to fit in the general setting, the state-space representation of the perturbed system must be of the form

$$\dot{x} = A_p x + Bu = Ax + A_\delta \delta C_\delta x + Bu = Ax + A_\delta \omega + Bu$$
$$z = C_\delta x$$
$$y = Cx$$

with $\omega = \delta z \quad \omega \in \mathbf{R}$ and $\delta = [\delta_1 \quad \delta_2 \quad \delta_3]$. This is only possible if the matrix Δ has rank one, so it is necesary to choose between two sets of uncertain parameters m_2 c_2 or k. This fact motivated the choice of m_2 c_2 as uncertain parameters throughout the thesis. In that case

$$\Delta = \begin{bmatrix} 0 & 0 & 0 & 0 \\ 0 & 0 & 0 & 0 \\ 0 & 0 & 0 & 0 \\ \delta_1 & 0 & \delta_1 & \delta_2 \end{bmatrix}$$

$$A_\delta^T = [0 \quad 0 \quad 0 \quad 1]$$

$$\delta = [\delta_1 \quad \delta_2]$$

$$C_\delta = \begin{bmatrix} 1 & 0 & 1 & 0 \\ 0 & 0 & 0 & 1 \end{bmatrix}$$

obtaining

$$\begin{bmatrix} z \\ y \end{bmatrix} = \begin{bmatrix} C_\delta(sI - A)^{-1}A_\delta & C_\delta(sI - A)^{-1}B \\ C(sI - A)^{-1}A_\delta & C(sI - A)^{-1}B \end{bmatrix} \begin{bmatrix} \omega \\ u \end{bmatrix}$$

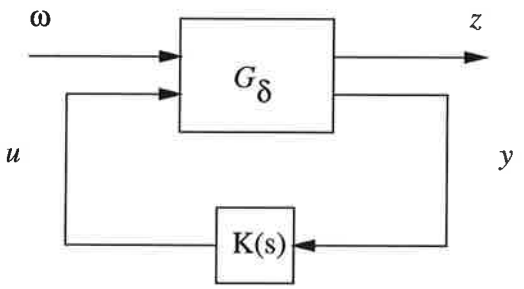

Figure 3.2: System representation

3.2 Parametric coprime factor descriptions

One consequence of the results in [9] is that coprime factor descriptions of uncertain systems can be extended for the SIMO and MISO cases to include

parametric uncertainty and yet allow robustness optimization by convex techniques. These plant descriptions are of the form

$$G_{\delta,\Delta} = \frac{\tilde{N}(s) + \delta\tilde{N}_\delta(s) + \Delta(s)\tilde{N}_\Delta(s)}{\tilde{M}(s) + \delta\tilde{M}_\delta(s) + \Delta(s)\tilde{M}_\Delta(s)}$$

where

- $\tilde{M}^{-1}\tilde{N}$ is the coprime factorization of a nominal transfer function.
- $\tilde{M}_\delta$,$\tilde{M}_\Delta$,$\tilde{N}_\delta$, $\tilde{N}_\Delta$ are all fixed known transfer matrices with elements in $\mathbf{RH}_\infty$.
- $\delta \in \mathbf{R}^m$ and $\Delta \in \mathbf{RH}_\infty$ are uncertain but bounded in norm.

Such a representation can be derived from a block diagram of the form

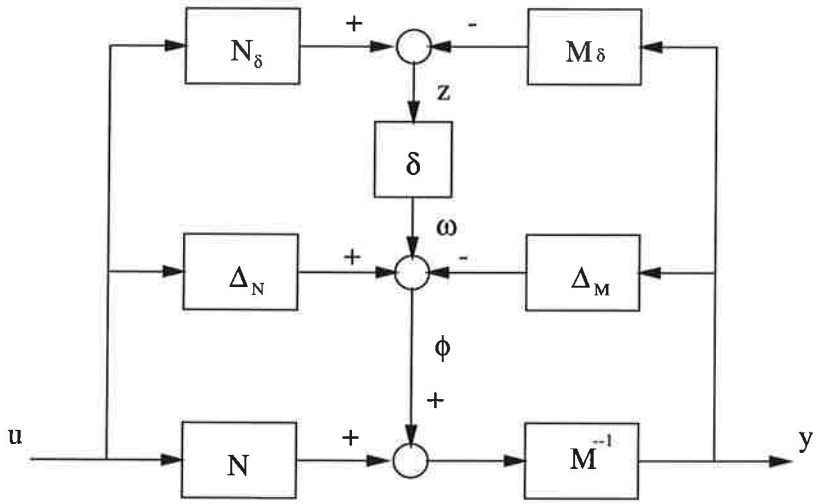

Figure 3.3: Parametric coprime factor description

the intermediate equations being

$$\begin{aligned} y &= \tilde{M}^{-1}(\tilde{N}u + \phi) \\ \phi &= \Delta_{\tilde{N}}u - \Delta_{\tilde{M}}y + \omega \\ \omega &= \delta z \\ z &= \tilde{N}_\delta u - \tilde{M}_\delta y \end{aligned}$$

The procedure to get $\tilde{N}$, $\tilde{M}$, $\tilde{N}_\delta$ and $\tilde{M}_\delta$ is explained in chapter 8.

Chapter 4

Previous designs

In this chapter several designs, taken from a previous thesis [2] on the same plant, are recalculated. The objective is to have a reference for the performance to be expected from subsequent controllers. The main idea is to get a closed-loop response to a step input which is as fast as possible but keeping overshooting below 5% or even to have no overshooting. All details of the designs can be found in [2] and here only the results are presented.

4.1 PI control

The plant has four poles: one at the origin, one on the negative real axis and two oscillatory poles just barely in the negative half plane. The PI adds one pole at the origin and a zero that can be placed anywhere on the real axis. The location of the zero will determine the location of the closed loop poles. The first idea is to move the two poles at the origin into the negative half plane but that also moves the pole on the negative real axis towards and eventually past the origin. One possible choice is to place all three poles at the same distance α from the origin. The two oscillatory poles of the process will then be almost unaffected and will not particularly influence the behaviour of the closed loop system. The three slow poles are placed at the same distance of the origin by setting the desired damping of the closed loop system. In addition, in order to reduce the overshoot of the step response only a fraction β of the reference signal acts on the proportional part of the controller. So the PI controller implemented is described by

$$u(s) = K_c(\beta r(s) - y(s)) + \frac{K_c}{sT_i}(r(s) - y(s))$$

and the expressions of K_c and T_i are

$$K_c = \frac{a^2\omega_p^2}{K_p(2\zeta + 1)}$$

$$T_i = \frac{(2\zeta + 1)^2}{a}$$

The value of β is set to $\beta = 0$. Below a table is shown with the values of K_c and T_i for three different values of the closed loop damping ζ.

ζ	K_c	T_i
0.3	18.9703	0.9639
0.5	15.1762	1.5060
0.7	12.6469	2.1687

Table 4.1: PI parameters

A comparison of the step response of all three resulting PIs is shown in figure 4.1 and the corresponding values of settling time and overshooting in table 4.2.

ζ	Overshooting %	Settling time t_s (sec)
0.3	23	5.2
0.5	8	4.5
0.7	0	4

Table 4.2: PI specifications

Accordingly with these results the PI for $\zeta = 0.7$ was chosen for comparison with subsequent controllers.

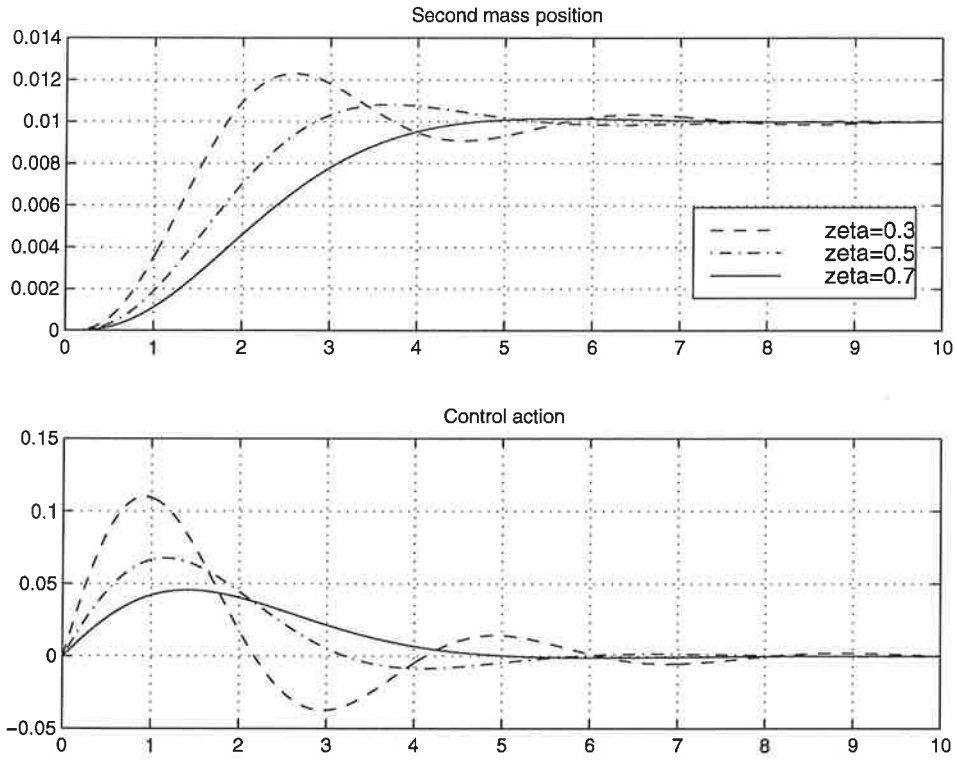

Figure 4.1: PI for various ζ

4.2 PID control

When using a PI controller the speed of the closed loop system was limited by the real pole at $s = -a$. With a PID controller there is one extra zero which can be used to cancel this pole. The two poles at the origin can now be moved further into the negative half-plane, limited instead by the oscillatory poles which will move towards and eventually past the imaginary axis. In order to ensure the cancellation of the pole in $s = -a$ the parameters of the PID must fulfill the following condition

$$T_i = \frac{aT_d - N}{a(aT_d(N+1) - N)}$$

In addition, the influence of the reference signal on both the proportional and the derivative part of the controller are weighted with parameters β and γ to reduce overshooting. So the implemented PID controller is described

by

$$u(s) = K_c\Big(\beta + \frac{1}{sT_i} + \gamma\frac{sT_d}{1+\frac{sT_d}{N}}\Big)r(s) - K_c\Big(1 + \frac{1}{sT_i} + \frac{sT_d}{1+\frac{sT_d}{N}}\Big)y(s)$$

The parameter N is set to $N = 10$, which is a usual value, and $\beta = \gamma = 0$.The other parameters were chosen to be $K_c = 30$ and $T_d = 0.25$, so $T_i = 1.3038$. The response to a step input of amplitude 0.01 compared to that of the PI for $\zeta = 0.7$ is shown in figure 4.2, and the corresponding values of settling time and overshooting in table 4.3.

Controller	Overshooting %	Settling time t_s (sec)
PID	4	2.4
PI	0	4

Table 4.3: PID specifications

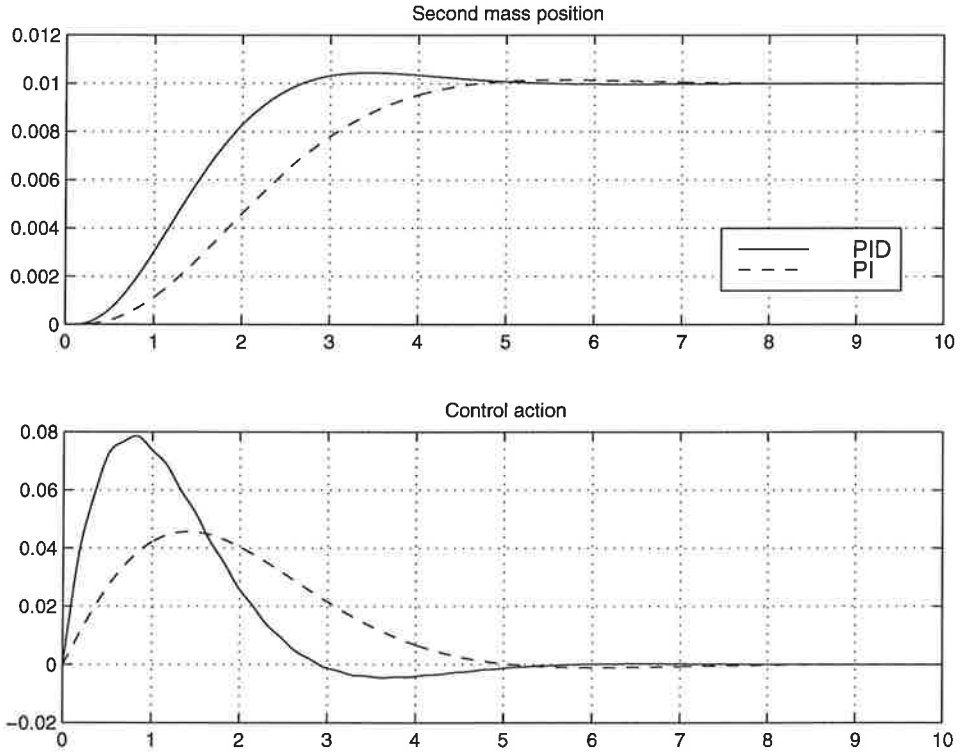

Figure 4.2: PID and PI compared

4.3 2 D.O.F. LQG plus feedforward

The controller described in this section has a structure with separate feedback and feedforward parts. The feedback part has two degrees of freedom, that is, reference and measured signal are processed separately. Besides that, it uses state feedback, consequently it uses more information about the process than PID control. The reference is introduced through a reference model which gives a "desired state" that in turn is compared with the estimated state. This "state error" is fed to the constant matrix gain. Additionally the observer, a Kalman filter , uses an extended state vector in order to introduce integral action as explained below. The general structure is presented in figure 4.3.

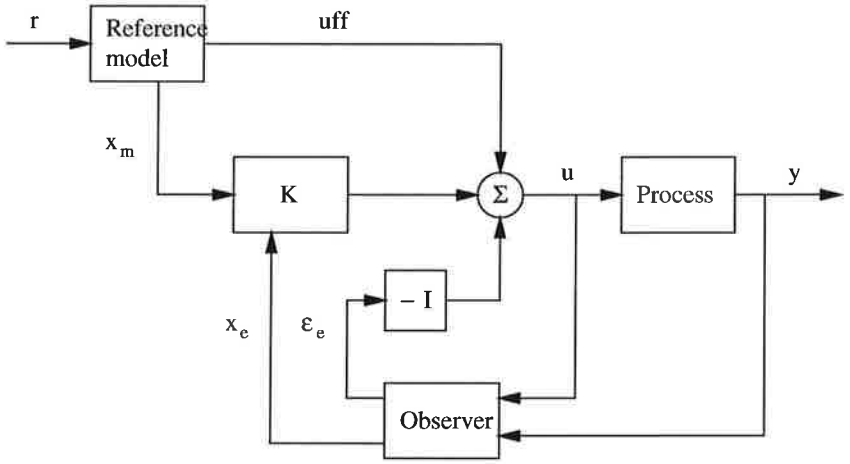

Figure 4.3: Controller structure

4.3.1 LQG state feedback

The process model is

$$\dot{x}(t) = Ax(t) + Bu(t) + B_\xi \xi(t)$$
$$y(t) = Cx(t) + e(t)$$

where $\xi(t)$ and $e(t)$ are stochastic disturbances. B_ξ is equal to B, so the state noise is considered to be entering the system in the same way as the control signal. The cost function to be minimized is

$$J = E\Big\{ \sum_{k=0}^{N-1} \left[x^T(t)Q_{1c}x(t) + 2x^T(t)Q_{12c}u(t) + u^T(t)Q_{2c}u(t)\right]dt + x^T(Nh)Q_{0c}x(Nh)\Big\}$$

The design parameters are Q_{1c}, Q_{12c}, Q_{2c} and , for the kalman filter design, the approximated disturbance covariances σ_e^2 and σ_v^2. The meaning of $\sigma_v^2$is explained below. Since only the steady state solution of the corresponding Riccati equation is used, the parameter Q_{0c} doesn't have to be set.

Disturbances $\xi(t)$ and $e(t)$ can be considered as white noise with zero mean value and covariances σ_v^2 and σ_e^2. However, this structure will not be able to eliminate errors due to constant disturbances. If instead $\xi(t)$ is considered to be the integral of a white noise $v(t)$ with zero mean value and covariance σ_v^2 the process model will be

$$\begin{aligned}\dot{x}(t) &= Ax(t) + Bu(t) + B_\xi\xi(t)\\ \dot{\xi}(t) &= v(t)\\ y(t) &= Cx(t) + e(t)\end{aligned}$$

Constant disturbances can be compensated by substracting from the control signal a term $B^{-1}B_\xi\hat{\xi}(t)$, since the disturbance can't be measured directly. The estimate of the disturbance ξ is obtained using an extended state vector $x^T = [x(t) \quad \xi(t)]$ in the Kalman filter.

4.3.2 The reference model

The first mass is modelled as a second order system independent of the second mass and with the reference signal r as its input. The transfer function from the reference signal to the position x_1^m is

$$G_{m1} = \frac{\alpha^2}{(s+\alpha)^2}$$

where α is a design parameter setting the speed of the model. Similarly the second mass is regarded as a second order system with the position of the first mass as as its input. The transfer function from x_1^m to the second mass position x_3^m is

$$G_{m2} = \frac{\beta^2}{(s+\beta)^2}$$

where β is another design parameter. The reference model can be expressed as a state space system

$$\dot{x}_m = A_m x_m + B_m r$$

where, using a weighted state vector $x^T = [y_1 \ \sqrt{\frac{m_1}{k}}\dot{y}_1 \ y_2 \ \sqrt{\frac{m_2}{k}}\dot{y}_2]$, we have

$$A = \begin{bmatrix} 0 & \sqrt{\frac{k}{m_1}} & 0 & 0 \\ -\alpha^2\sqrt{\frac{m_1}{k}} & -2\alpha & 0 & 0 \\ 0 & 0 & 0 & \sqrt{\frac{k}{m_2}} \\ \beta^2\sqrt{\frac{m_2}{k}} & 0 & -\beta^2\sqrt{\frac{m_2}{k}} & -2\beta \end{bmatrix}$$

$$B^T = \begin{bmatrix} 0 & \alpha^2\sqrt{\frac{m_1}{k}} & 0 & 0 \end{bmatrix}$$

4.3.3 The feedforward

The feedforward control signal u_{ff} is created from

$$u_{ff} = \frac{G_{m1}}{\bar{G}_p} r$$

$\bar{G}_p$ is chosen to be a simplified process model transfer function

$$\bar{G}_p = \frac{b}{s(s+a)}$$

where $b = \frac{K_p}{\omega_p^2}$. The signal u_{ff} can then be expressed in terms of x_m and r as

$$u_{ff} = -\frac{\alpha^2}{b} x_1^m + \frac{a - 2\alpha}{\sqrt{\frac{m_1}{k}}} x_2^m + \frac{\alpha^2}{b} r$$

and in state space form

$$\begin{aligned} \dot{x}_m &= A_m x_m + B_m r \\ r &= C_m x_m + D_m r \end{aligned}$$

with A_m and B_m as above and

$$C_m = \begin{bmatrix} -\frac{\alpha^2}{b} & \frac{a-2\alpha}{\sqrt{\frac{m_1}{k}}} & 0 & 0 \end{bmatrix}$$

$$D_m = \begin{bmatrix} \frac{\alpha^2}{b} \end{bmatrix}$$

4.3.4 Nominal designs

Two designs have been tested, the corresponding parameters are summarized in table 4.4. Then the response of both controllers to a step input is compared to that of the PID.

"LQG+I+FF"	Q_{1c}	Q_{2c}	Q_{12c}	σ_e	σ_v	α	β
(a)	100I	I	0	0.00001	1	2	6
(b)	750I	I	0	0.00001	1	3	6

Table 4.4: "LQG+I+FF" parameters

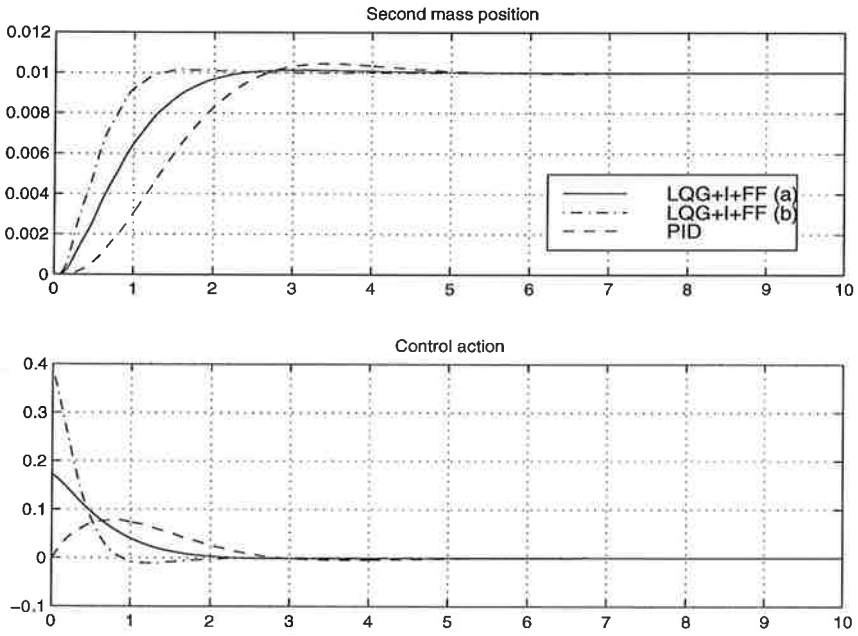

Figure 4.4: "LQG+I+FF" and PID compared

Controller	Overshooting %	Settling time t_s (sec)
LQG+I+FF (a)	1	1.9
LQG+I+FF (b)	2	1.1
PID	4	2.4

Table 4.5: LQG specifications

Chapter 5

Mixed sensitivity $\mathcal{H}_\infty$ control

In this chapter, and the following, the design strategy is to directly shape the magnitudes of closed loop transfer functions such as the sensitivity function $S(s)$ and the complementary sensitivity $T(s)$. This strategy is formulated as an $\mathbf{H}_\infty$ optimal control problem and our main task will be to select reasonable bounds on the desired closed loop transfer functions. Since $S + T = I$, one may think it is enough to minimize the norm

$$\|w_p S\|_\infty < 1$$

where w_p is a weighting function. However, this specification only puts a lower bound on the bandwidth, but not an upper one and doesn't allow to specify the roll-off of $L(s)$ above the bandwidth. In addition there is no restriction of the magnitude of control signals except if the plant has a RHP-zero. In that case the stability requirement would indirectly limit the controller gains. For these reasons the norm

$$\left\| \begin{matrix} w_p S \\ w_u K S \end{matrix} \right\|_\infty < 1$$

is considered. The term $w_u K S$ puts a restriction on the magnitude of the control action and $T(s)$ is indirectly shaped since $T = GKS$.

5.1 Weight selection

Typical specifications in terms of S are

1. Minimum bandwidth frequency ω_B^*.
2. An upper bound A for the magnitude of S at low frequencies.
3. Maximum peak magnitude of S, $\|S(j\omega)\|_\infty \leq M$.

These specifications may be captured by an upper bound $\frac{1}{|w_p(s)|}$ on the magnitude of S where

$$w_p(s) = \frac{\frac{s}{M} + \omega_B^*}{s + \omega_B^* A}$$

The above mentioned upper bound is equal to $A \leq 1$ at low frequencies, equal to $M \geq 1$ at high frequencies and the asymptote crosses one at the frequency ω_B^*. If a steeper slope for L (and S) below the bandwidth is desired, the following weight may be used

$$w_p(s) = \frac{(\frac{s}{\sqrt{M}} + \omega_B^*)^2}{(s + \omega_B^* \sqrt{A})^2}$$

As for KS, the weight w_u may be a constant or if we want to ensure K is small outside the system bandwidth we may take

$$w_u(s) = \frac{1 + \tau_1 s}{1 + \tau_2 s} \quad \text{where } \tau_2 \ll \tau_1$$

5.2 Nominal design

For the parameters of the weight w_p the following values have been chosen: $M = 2$, $\omega_B^* = 2$ and $A = 0.0001$. When choosing w_u we want a high control gain for frequencies below ω_B^* and to make sure the gain is small for frequencies over ω_B^*, particularly because it is important not to excite the resonant mode of the plant. First the weight

$$w_u = \frac{s + 10}{s + 1000}$$

was tried, but to get better performance it was necessary to use a higher order weight. After several trials the final weight was chosen as

$$w_u = \frac{200(s + 5)(s + 10)}{(s + 1000)^2}$$

The bode plots of both weigths are shown in figure 5.2. The response to a step input of the resulting closed loop system as well as bode plots of the S, T and KS are shown in figures 5.1 to 5.6. Table 5.1 shows the data of the comparison between the mixed sensitivity design and the fastest LQG+I+FF controller. The transfer function of the controller is

$$K = \frac{0.9052\, s\, (s + 2.656)(s + 1000)^2(s^2 + 2.74s + 390.8)}{(s + 0.0002)(s + 12.24)(s + 160.6)(s^2 + 10.65s + 66.49)(s^2 + 2.606s + 388)}$$

and can be simplified to

$$K = \frac{5636\, s\, (s + 2.656)}{(s + 0.0002)(s + 12.24)(s^2 + 10.65s + 66.49)}$$

as it is seen in the bode plot of figure 5.3. The controller obtained is very good in theory, but since the real plant has a dead zone we need to have integral action in the controller. For our plant, this is not possible with this technique because it introduces pole-zero cancellations between the plant and the controller and in particular the controller always has a zero in the imaginary axis to cancel the integrator of the plant. This zero compensates with the pole $(s + 0.0002)$ included in the weight w_p to introduce integral action in the controller. For this reason the next step is to try with $\mathbf{H}_\infty$ loop-shaping techniques. These will be treated in Chapter 6.

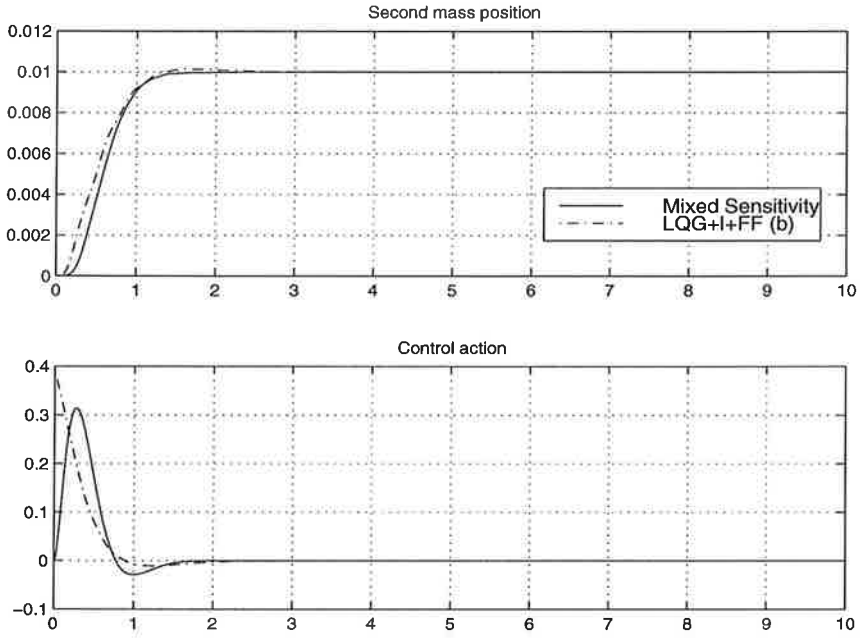

Figure 5.1: Mixed sesitivity and LQG+I+FF (b) compared

Controller	Overshooting %	Settling time t_s (sec)
Mixed Sens.	0	1.1
LQG+I+FF (b)	2	1.1

Table 5.1: Mixed sesitivity controller specifications

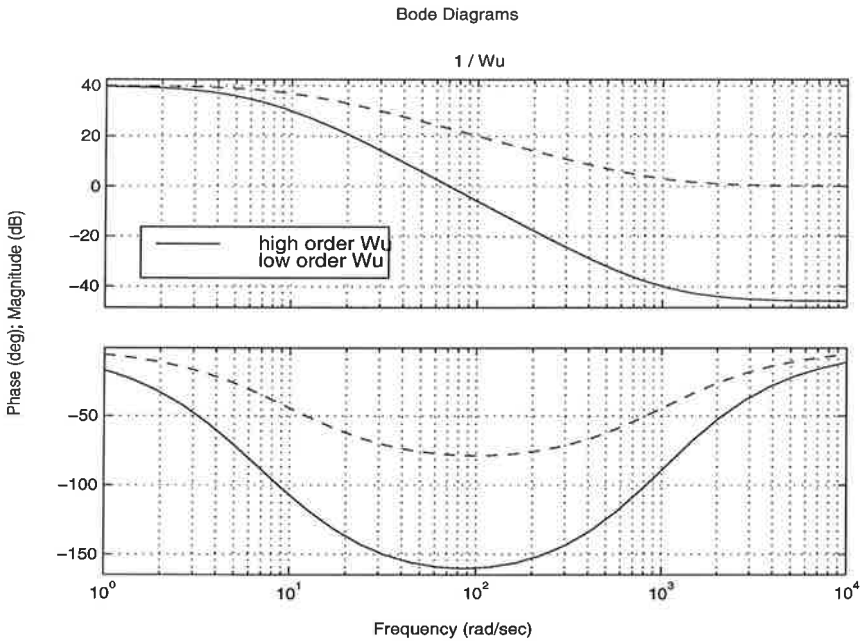

Figure 5.2: Weights on KS

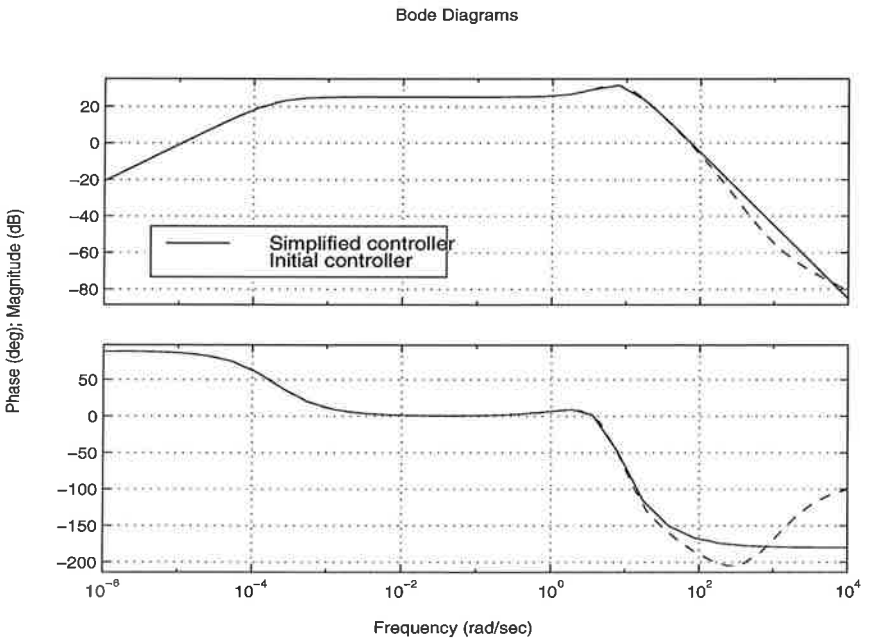

Figure 5.3: Simplified controller

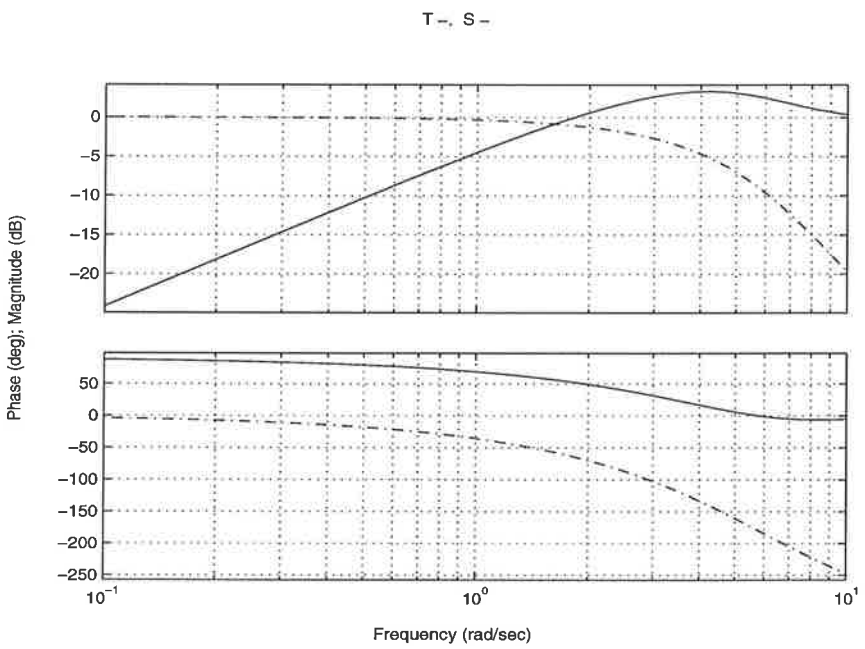

Figure 5.4: S and T functions

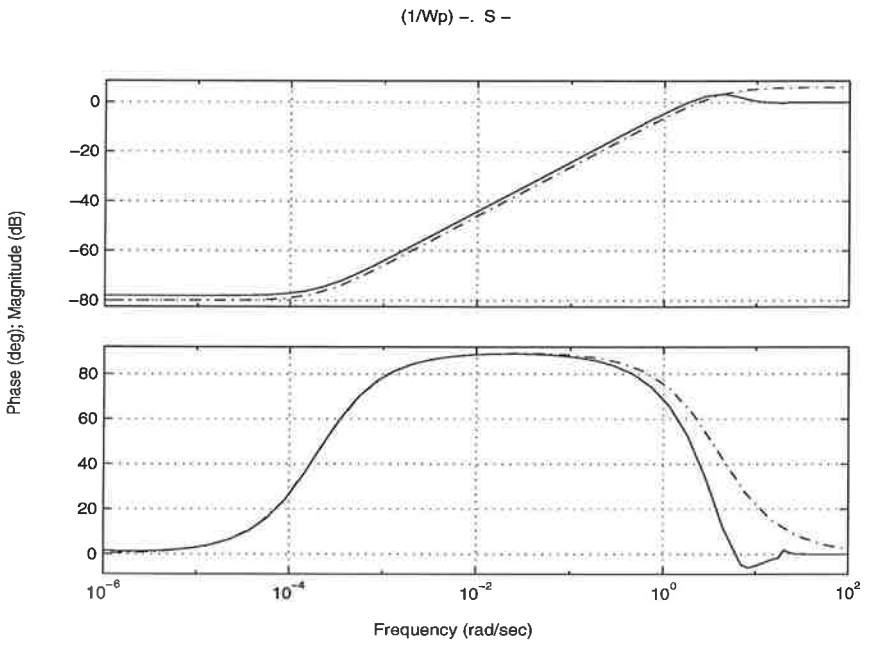

Figure 5.5: S and $\frac{1}{w_p}$

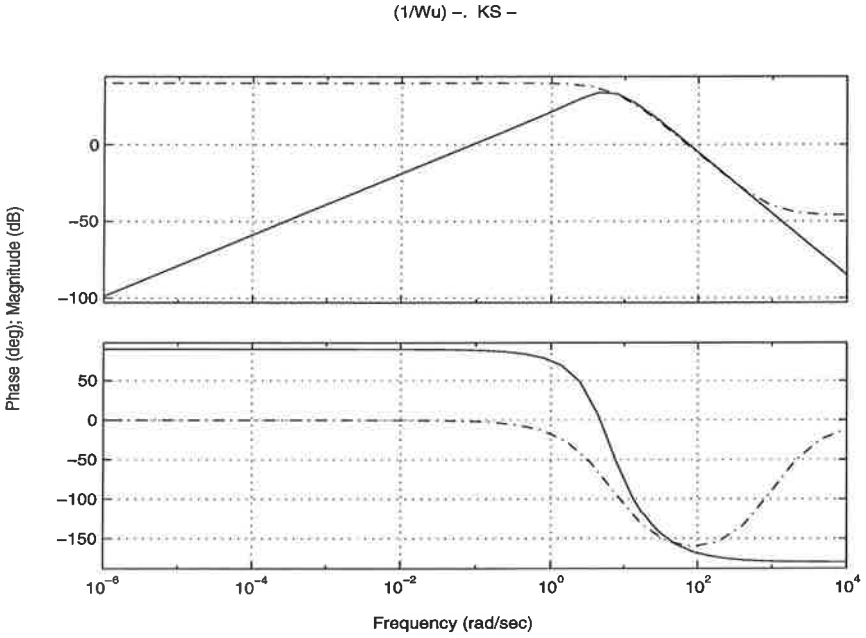

Figure 5.6: KS and $\frac{1}{w_u}$

Chapter 6

$\mathcal{H}_\infty$ loop-shaping design

The loop-shaping design procedure used in this chapter is based on $\mathcal{H}_\infty$ robust stabilization combined with classical loop shaping. First, the open-loop plant is augmented by a pre-compensator to give a desired shape to the open-loop frequency response . Then the resulting shaped plant is robustly stabilized with respect to coprime factor uncertainty using $\mathcal{H}_\infty$ optimization. If W_1 is the pre-compensator then the shaped plant is given by

$$G_s = GW_1$$

The controller K_s is synthesized by solving a robust stabilization problem for the shaped plant G_s with a normalized left coprime factorization $G_s = M_s^{-1}N_s$ as explained in [8] or in [10]. The feedback controller for the plant G is then $K = W_1K_s$. One of the advantages of this method is that, except for special systems with all-pass factors, it doesn't introduce pole-zero cancellations between the plant and the controller.

6.1 1 D.O.F controllers

In this section one degree of freedom controllers are developed.First, the pre-compensator must be chosen. In general it would include integral action for low frequency performance, phase-advance for reducing roll-off rates at crossover, and phase-lag to increase the roll-off rates at high frequencies. The simplest pre-compensator would be of the form

$$W_1 = \frac{K_w(s+a)}{s\,(s+b)}$$

By trial and error, and also looking at the mixed sensitivity controller developed in Chapter 5, the values $K_w = 200$, $a = 2.656$ and $b = 12.24$ are chosen. The resulting transfer function is

$$W_1 = \frac{200(s+2.656)}{s\,(s+12.24)} \tag{6.1}$$

This pre-compensator is very simple, but the roll-off at the crossover region of GW_1 is of 40 dB / decade whereas a desirable roll-off rate would be of 20 dB / decade. For this reason a higher order pre-compensator was designed

$$W_1 = \frac{900(s+1)^2}{s\,(s+8)^2} \tag{6.2}$$

Both pre-compensators have been tried. The bode plots of the corresponding shaped plants are in figure 6.1.

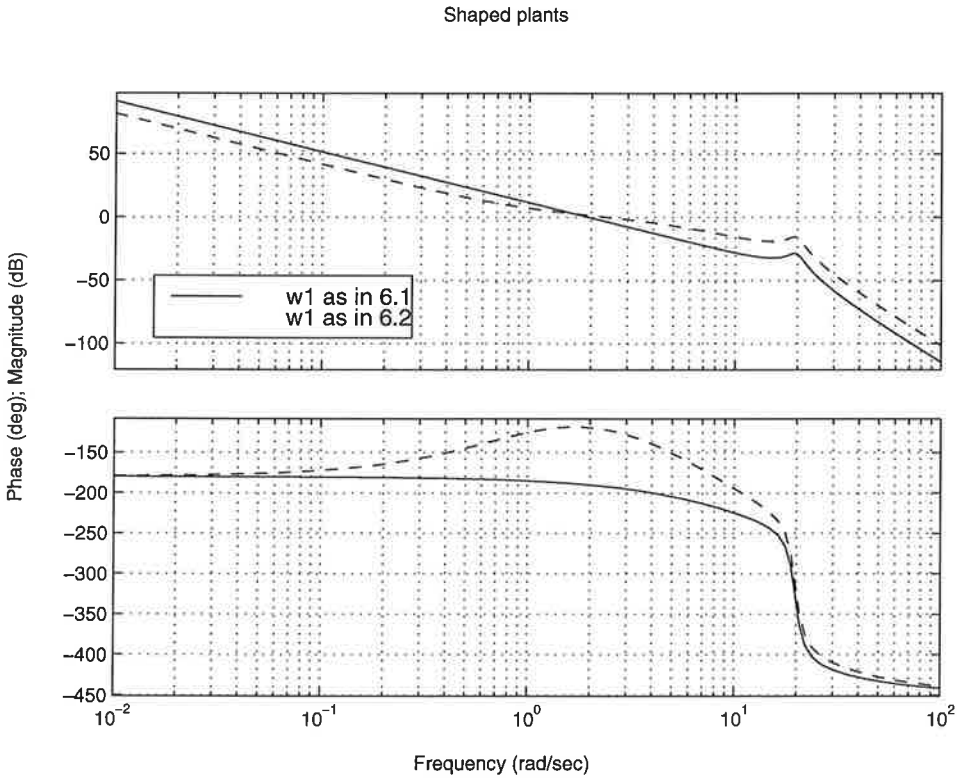

Figure 6.1: Shaped plants

The bode plots of the corresponding feedback controllers $K = W_1 K_s$ compared to that of the mixed sensitivity controller are in figure 6.3 and 6.4. For implementing the controller the configuration shown in figure 6.2 has been found useful when compared with the conventional set up.

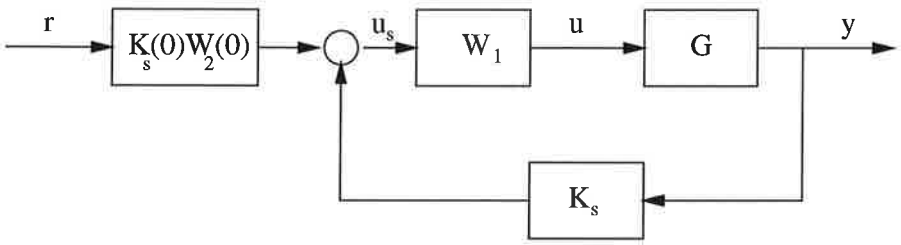

Figure 6.2: Implementation of the loop-shaping controller

This is because the references don't directly excite the dynamics of K_s, which can result in large amounts of overshoot (classical derivative kick). The constant prefilter ensures a steady-state gain of 1, assuming integral action in W_1 or G. The response of the controllers to an input step is shown in figures 6.5 and 6.6. The values of the overshooting and settling time corresponding to these simulations are in table 6.1,where

1. Controllers (a , a^*) have been designed using 6.1, and controllers (b , b^*) using 6.2.
2. The (*) indicates the controller is implemented in the conventional way and (a , b) have been implemented using the special setup to avoid large overshooting.

Controller	Overshooting %	Settling time t_s (sec)
a^*	43	3
a	2	2.1
b^*	15	4.7
b	0	2.7

Table 6.1: 1 D.O.F Loop-shaping controller specifications

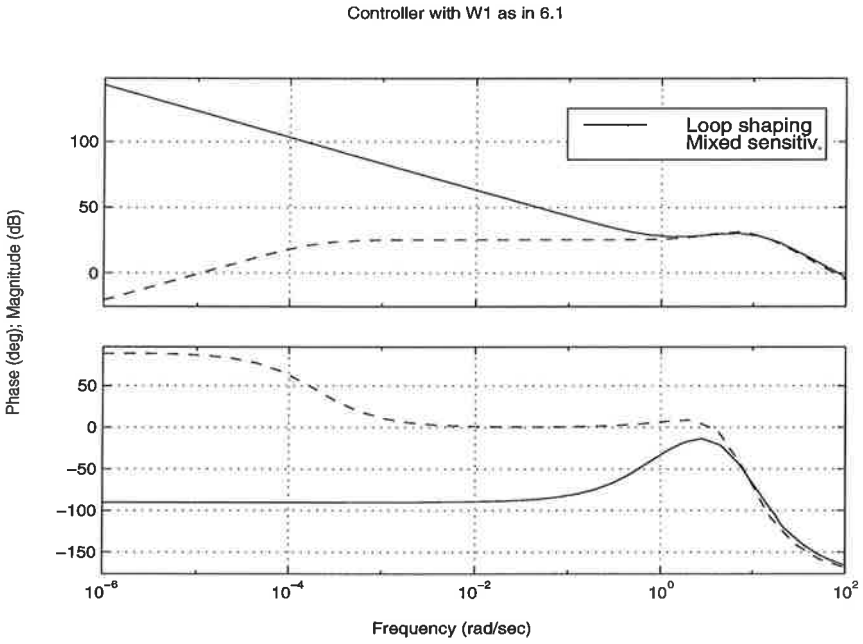

Figure 6.3: 1 D.O.F Loop-shaping controller (a)

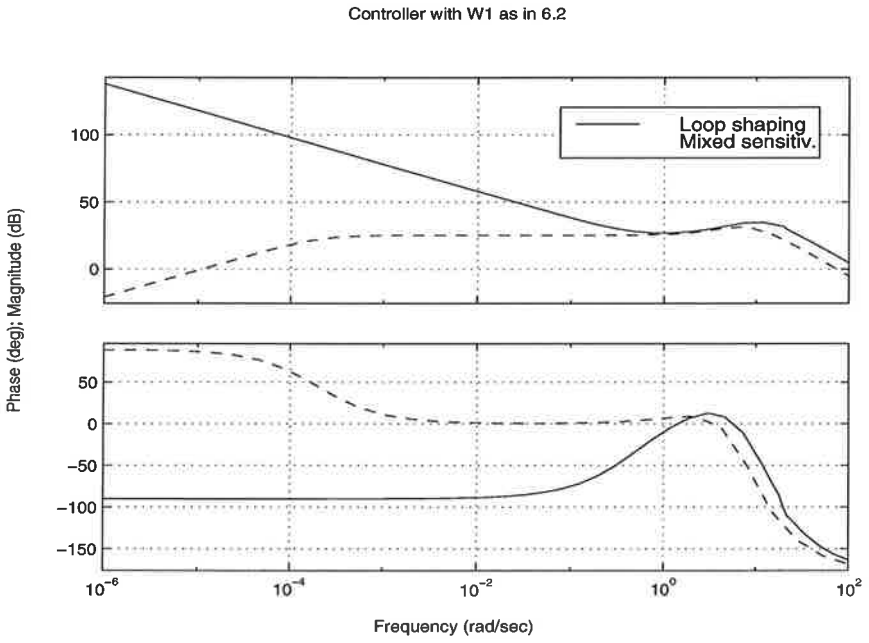

Figure 6.4: 1 D.O.F Loop-shaping controller (b)

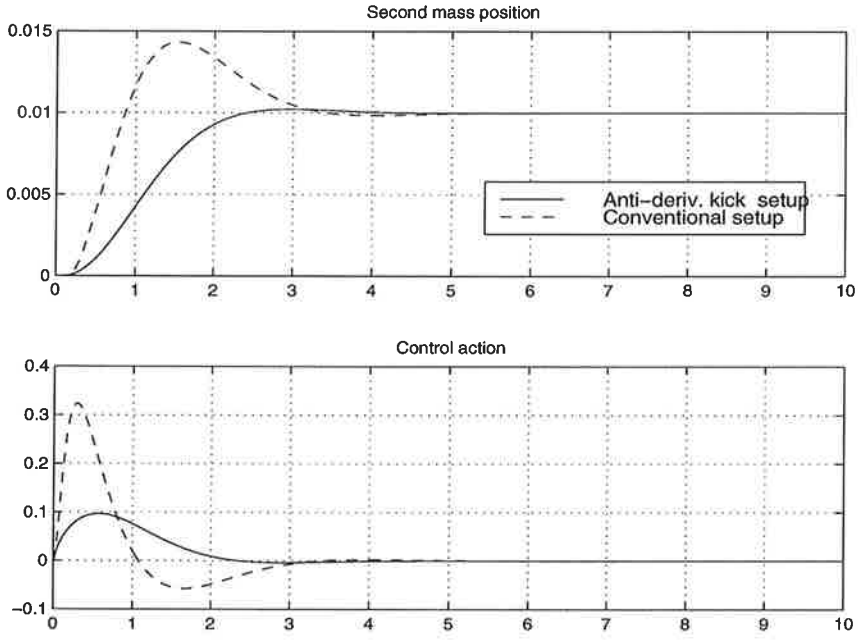

Figure 6.5: 1 D.O.F Loop-shaping controller (a)

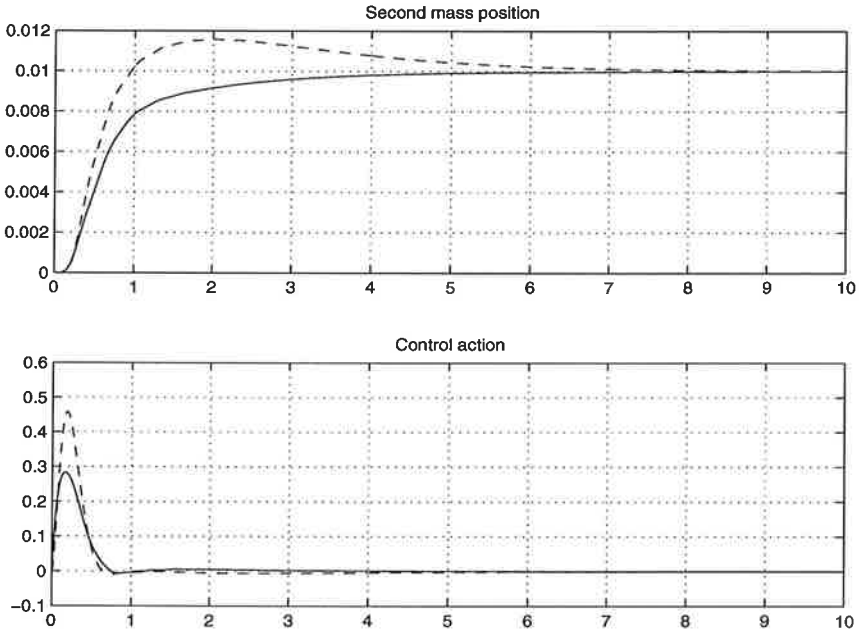

Figure 6.6: 1 D.O.F Loop-shaping controller (b)

6.2 2 D.O.F controllers

In this section a two degrees of freedom controller is developed. The scheme used for this purpose is proposed in [10]. The feedback part of the controller is designed to meet robust stability and disturbance rejection requirements in a manner similar to the one degree of freedom loop-shaping design procedure. An additional prefilter part of the controller is then introduced to force the response of the closed-loop system to follow that of a specified reference model T_{ref}. Both parts of the controller are synthesized by solving the design problem illustrated in figure 6.7.

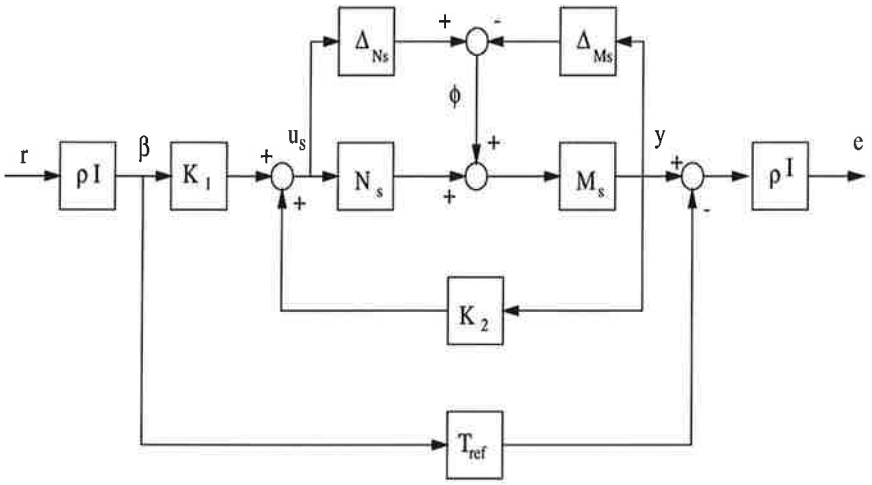

Figure 6.7: 2 D.O.F $\mathbf{H}_\infty$ loop-shaping design problem

The design problem is to find the stabilizing controller $K = [K_1 \; K_2]$ for the shaped plant $G_s = GW_1$ with a normalized coprime factorization $G_s = M_s^{-1}N_s$, which minimizes the $\mathbf{H}_\infty$ norm of the transfer function between the signals $[r^T \; \phi^T]^T$ and $[u_s^T \; y^T \; e^T]^T$. The problem can be cast into the general control configuration and solved suboptimally using standard methods and γ-iteration. The control signal to the shaped plant u_s is given by

$$u_s = \begin{bmatrix} K_1 & K_2 \end{bmatrix} \begin{bmatrix} \beta \\ y \end{bmatrix}$$

where K_1 is the prefilter, K_2 is the feedback controller, β is the scaled reference, and y is the measured output. The purpose of the prefilter is to ensure that

$$\|(I - G_s K_2)^{-1} G_s K_1 - T_{ref}\|_\infty \leq \gamma \rho^{-2}$$

6.2.1 Nominal designs

The main steps to synthesize a two degrees-of-freedom $\mathbf{H}_\infty$ loop-shaping controller are :

1. Design a one degree of freedom controller as in the previous section, hence W_1.
2. Select a desired closed-loop transfer function T_{ref} between the commands and controlled outputs.
3. Set the scalar parameter ρ to a small value greater than 1; for example something in the range 1 to 3.
4. Solve the $\mathcal{H}_\infty$ optimization problem to get $K = [K_1\ K_2]$.
5. To give exact model-matching at steady-state, replace the prefilter K_1 by $K_1 W_i$ where

$$W_i = [(I - G_s(0)K_2(0))^{-1}G_s(0)K_1(0)]^{-1}T_{ref}(0)$$

In this section two prefilters, those designed in the previous one, are tried

$$W_1 = \frac{200(s + 2.656)}{s\,(s + 12.24)} \qquad \text{(a)}$$

and

$$W_1 = \frac{900(s + 1)^2}{s\,(s + 8)^2} \qquad \text{(b)}$$

The reference model was at first the same as that in section 4.3 with $\alpha = 3$ and $\beta = 6$, but it turned out to be too slow so it was changed to

$$T_{ref}(s) = \frac{\alpha^2\beta^2\frac{1}{3}(s + 3)}{(s + \alpha)^2(s + \beta)^2} \qquad (6.3)$$

where $\alpha = 4$ and $\beta = 6$. The response to a step input of both reference models can be seen in figure 6.8. Finally the scalar parameter ρ is taken as $\rho = 3$ in both cases. The response to a step input of the 2 D.O.F $\mathbf{H}_\infty$ loop-shaping controllers, compared to that of the "LQG+I+FF" (b), is shown in figures 6.9 and 6.10.

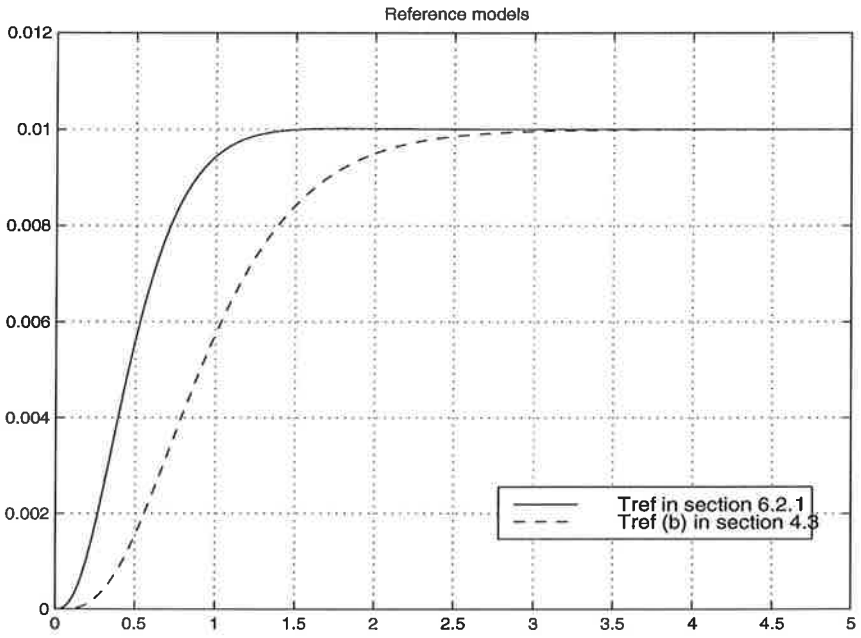

Figure 6.8: Reference models

Controller	Settling time t_s (sec)	Overshooting %
2 d.o.f LS (a)	1.2	0
2 d.o.f LS (b)	2.0	0
"LQG+I+FF" (b)	1.1	2

Table 6.2: 2 D.O.F Loop shaping controller specifications

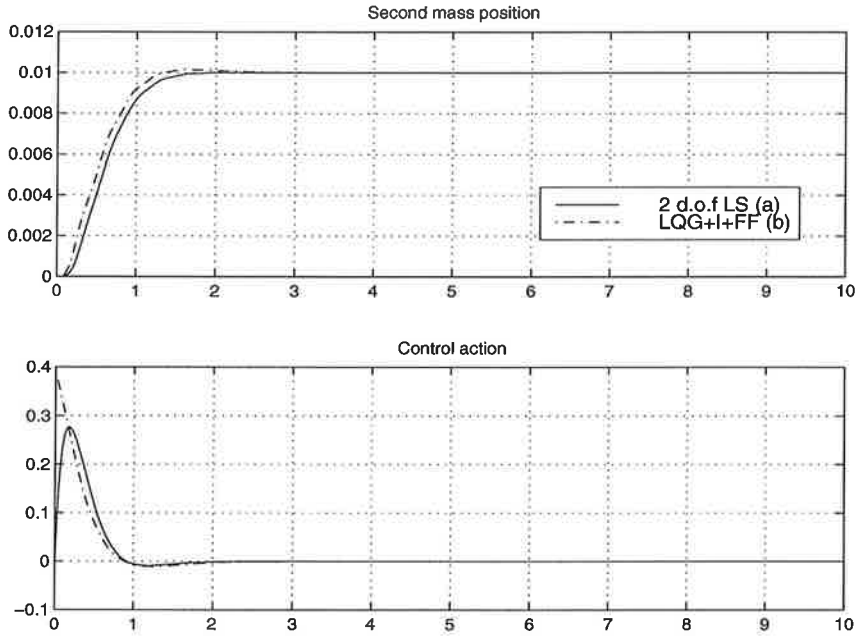

Figure 6.9: 2 D.O.F loop shaping controller (a) and "LQG+I+FF" (b) compared

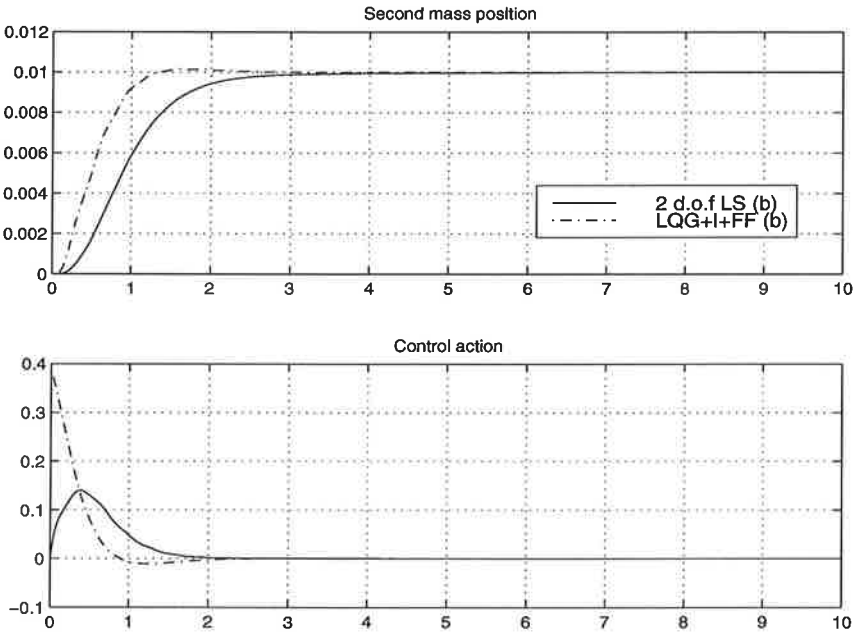

Figure 6.10: 2 D.O.F loop shaping controller (b) and "LQG+I+FF" (b) compared

Chapter 7

Robust performance : a comparison

In previous chapters the design of various controllers has been described, as well as their performance when simulated with the nominal plant. In this chapter we show the results of a series of simulations in which the values of the plant parameters m_2 and c_2 are varied. First the controllers with similar or comparable nominal performance are grouped. This classification is shown in table 7.1.

Controller	Settling time t_s (sec)	Overshooting %	Group
PI	4	0	1
PID	2.4	4	2
1 d.o.f LS (b)	2.7	0	"
LQG+I+FF (a)	1.9	1	3
2 d.o.f LS (b)	2	0	"
1 d.o.f LS (a)	2.1	2	"
LQG+I+FF (b)	1.1	2	4
Mixed Sens.	1.1	0	"
2 d.o.f LS (a)	1.2	0	"

Table 7.1: Controller classification

7.1 Simulations

In this section the results for the different groups mentioned above are shown. In the tables the settling time (t_s) in seconds and the overshooting (os) in % are given for five different experiments :

1. (nominal) simulations with the nominal plant .
2. $(m_2 + 1.5)$ second mass is increased with 1.5 Kg .
3. $(m_2 - 1.5)$ second mass is decreased by 1.5 Kg .
4. $(c_2 + 3)$ second damping coefficient is increased by 3 N/ms .
5. $(c_2 - 3)$ second damping coefficient is decreased by 3 N/ms .

The experiments varying the mass would correspond with adding three brass weights to the second mass carriage or leaving it empty. As for the variations in c_2, similar ones may be achieved in the real plant manipulating the screw in the damper.

7.1.1 First group of controllers

This group only contains the PI, which is noticeably slower than the others. The following graphics show the behaviour of the perturbed closed loop system compared to the nominal one. The results are summarized in table 7.2.We can see the variations that more noticeably affect the behaviour of the system are those in c_2.

experiments	Settling time t_s (sec)	Overshooting %
nominal	4.0	0
m_2+1.5	3.7	3
m_2 -1.5	4.2	2
c_2+3	6.8	6
c_2 -3	4.3	0

Table 7.2: PI simulations

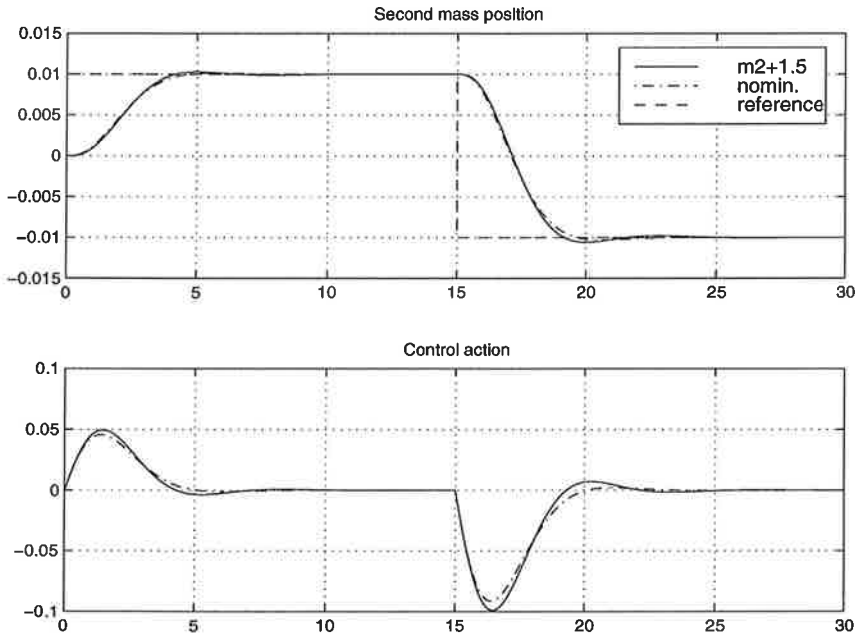

Figure 7.1: (1). Varying mass : m_2+1.5

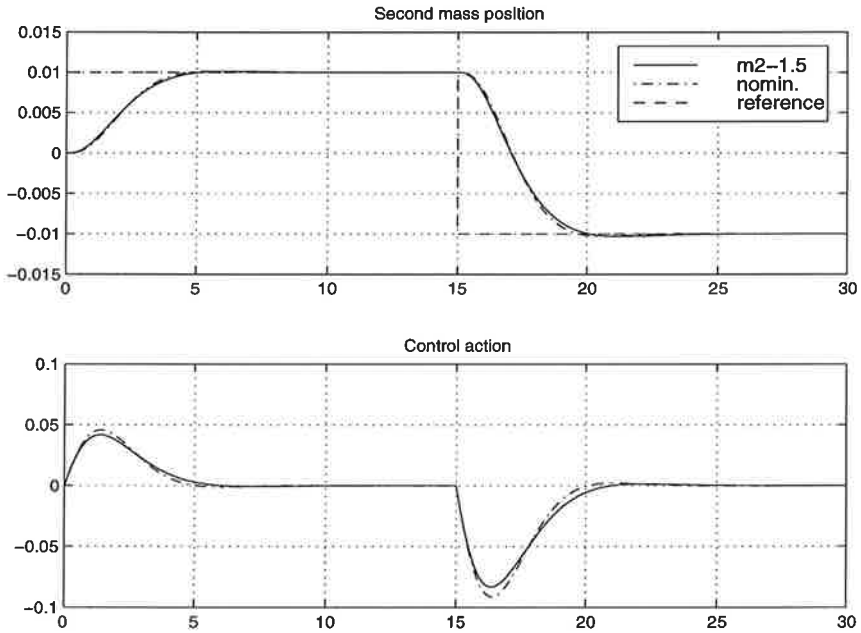

Figure 7.2: (1). Varying mass : m_2-1.5

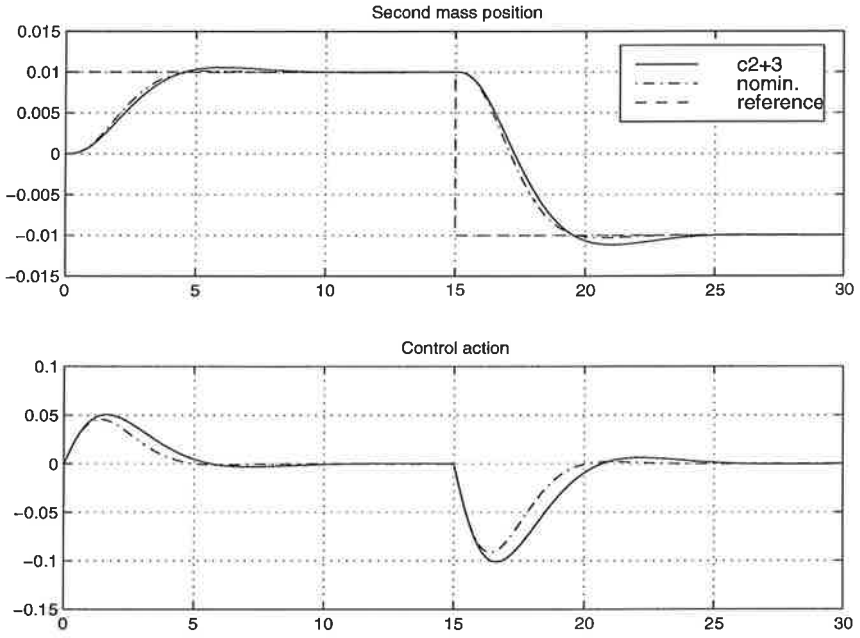

Figure 7.3: (1).Varying damping : c_2+3

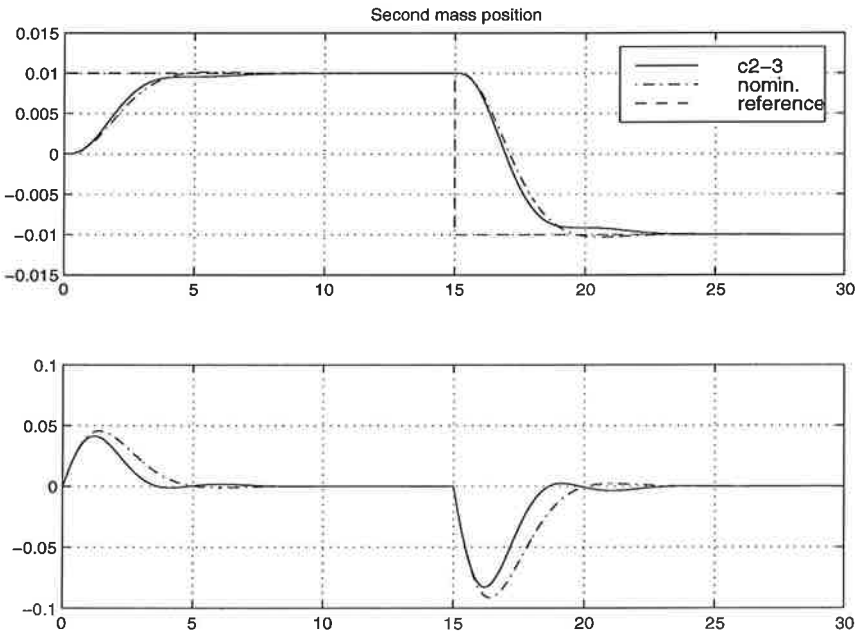

Figure 7.4: (1).Varying damping : c_2-3

7.1.2 Second group of controllers

In the second group, the controllers to be compared are the PID and the one degree-of-freedom loop-shaping controller designed with higher order weight (b). The following graphics show, for each experiment, the behaviour of the closed loop system for both controllers. The results are summarized in table 7.3. We can see that in general the loop shaping controller is better than the PID, except for the last case.

	nominal	m_2+1.5	m_2-1.5	c_2+3	c_2-3
PID	t_s=2.4 os=4	t_s=3.6 os=6	t_s=2.5 os=4	t_s=4.4 os=7	t_s=2.3 os=1
1 d.o.f LS (b)	t_s=2.7 os=0	t_s=1.8 os=0	t_s=2.9 os=0	t_s=2.6 os=1	t_s=3.8 os=(0)

Table 7.3: Second group of controllers

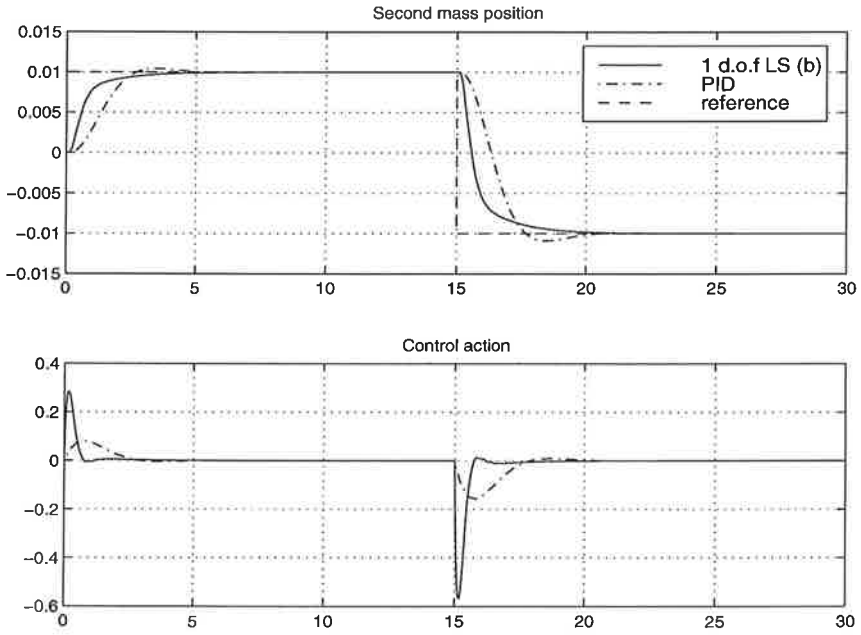

Figure 7.5: (2). Simulation with nominal plant

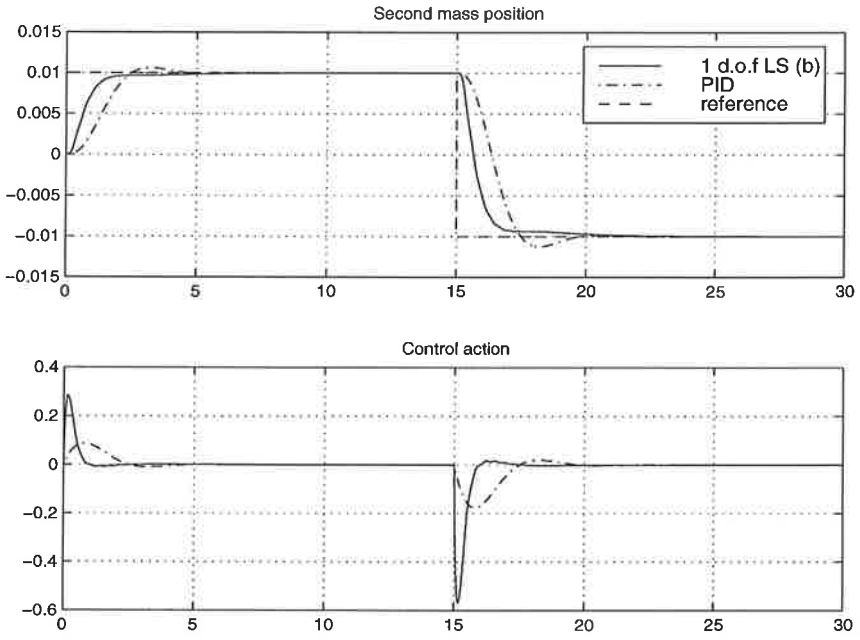

Figure 7.6: (2). Varying mass : m_2+1.5

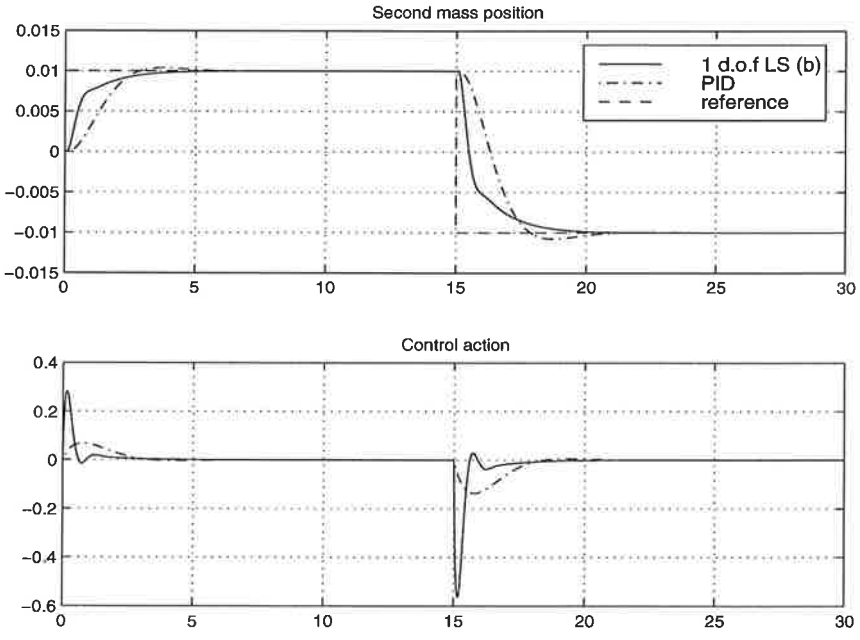

Figure 7.7: (2). Varying mass: m_2-1.5

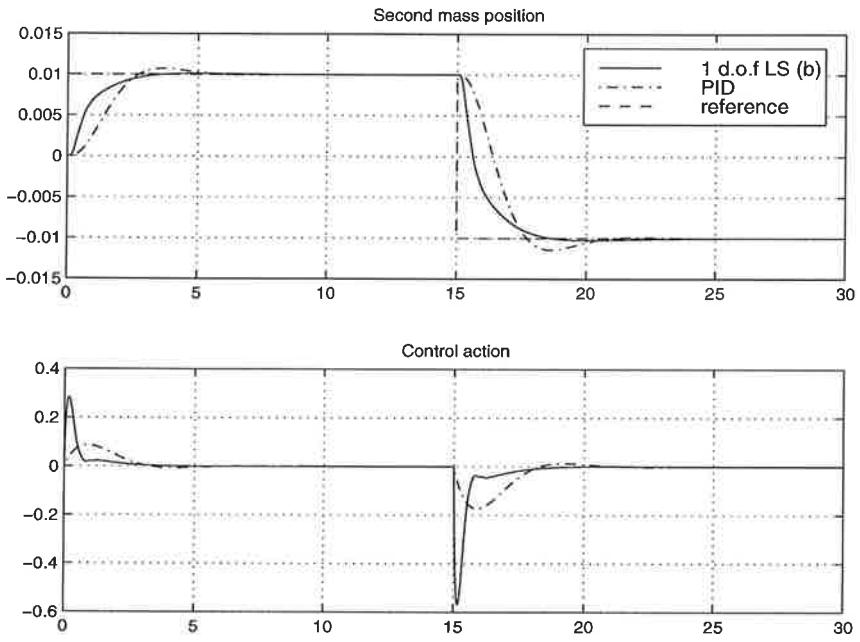

Figure 7.8: (2). Varying damping : c_2+3

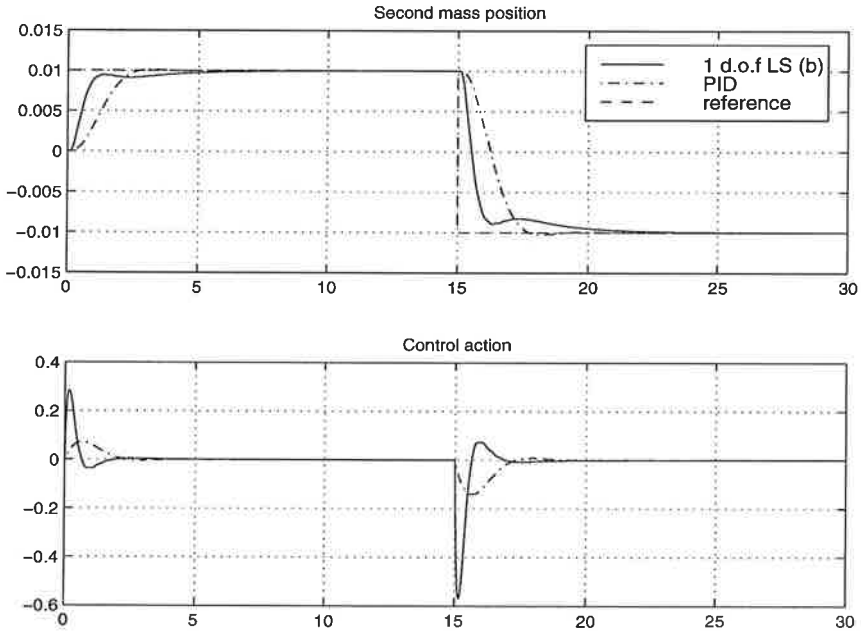

Figure 7.9: (2). Varying damping : c_2-3

7.1.3 Third group of controllers

In the third group, the controllers to be compared are the first "LQG+I+FF" with $Q = 100I$, the 2 D.O.F loop-shaping controller designed with the higher order weight (b), and the 1 D.O.F loop-shaping controller (a). Note the first two controllers in the list have two degrees of freedom. As can be seen in figures 7.11 to 7.14 and in table 7.4, their performance is equivalent. With the 2 D.O.F loop-shaping controller there is in all cases less overshooting but the settling time may be slightly bigger, except in the last case in which is clearly better than the "LQG+I+FF". As for the 1 D.O.F loop-shaping controller (figures 7.15 to 7.18), we can see in some cases its performance is comparable to that of its two degree-of-freedom counterparts but in general the behaviour of the perturbed closed loop system is worse.

	nominal	m_2+1.5	m_2-1.5	c_2+3	c_2-3
LQG+I+FF (a)	t_s=1.9 os=1	t_s=1.6 os=3	t_s=2.0 os=2	t_s=1.9 os=4	t_s=2.1 os=0
2 d.o.f LS (b)	t_s=2.0 os=0	t_s=1.8 os=1	t_s=2.4 os=0	t_s=2.3 os=2	t_s=1.7 os=0
1 d.o.f LS (a)	t_s=2.1 os=2	t_s=3.2 os=8	t_s=2.4 os=2	t_s=4.1 os=6	t_s=3.5 os=(0)

Table 7.4: Third group of controllers

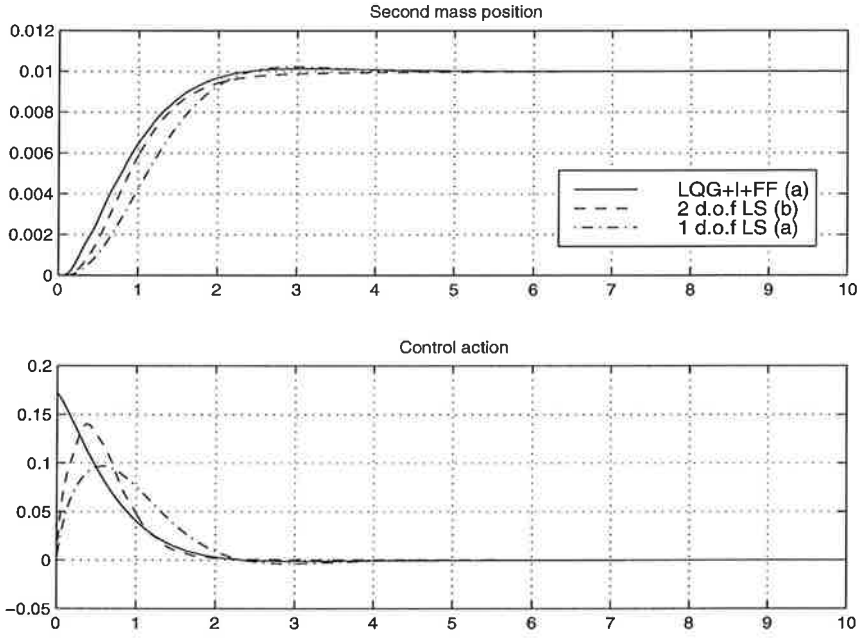

Figure 7.10: (3). Simulations with the nominal plant

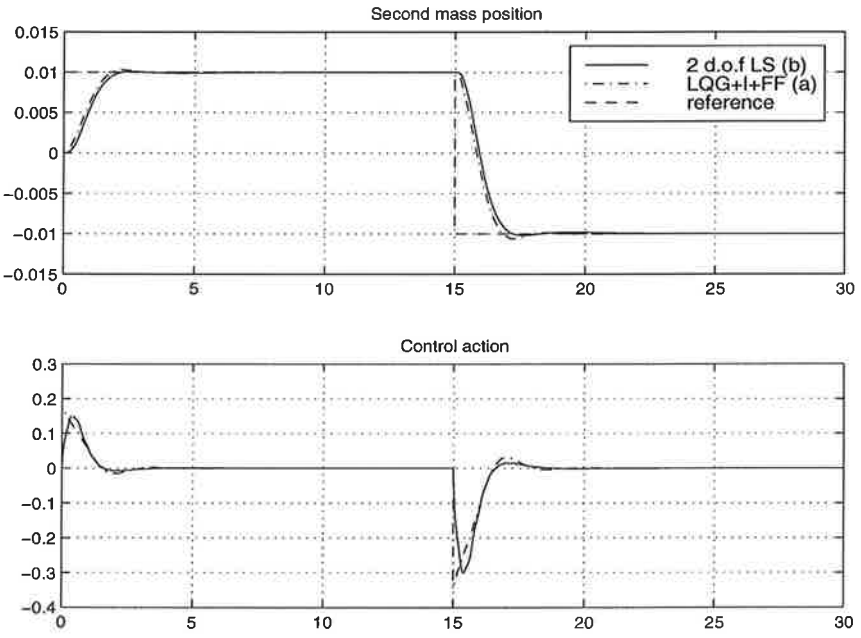

Figure 7.11: (3). Varying mass : m_2+1.5

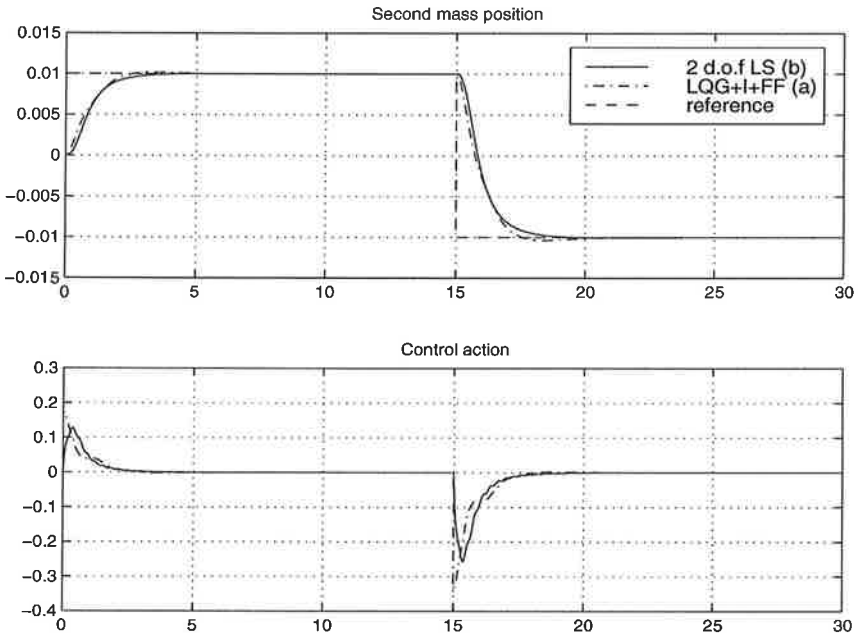

Figure 7.12: (3). Varying mass : m_2-1.5

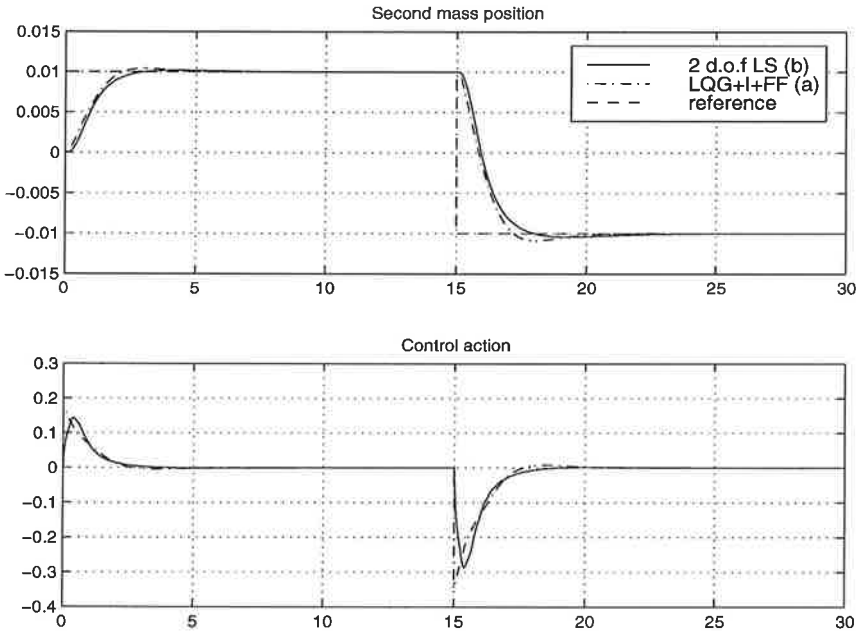

Figure 7.13: (3). Varying damping : c_2+3

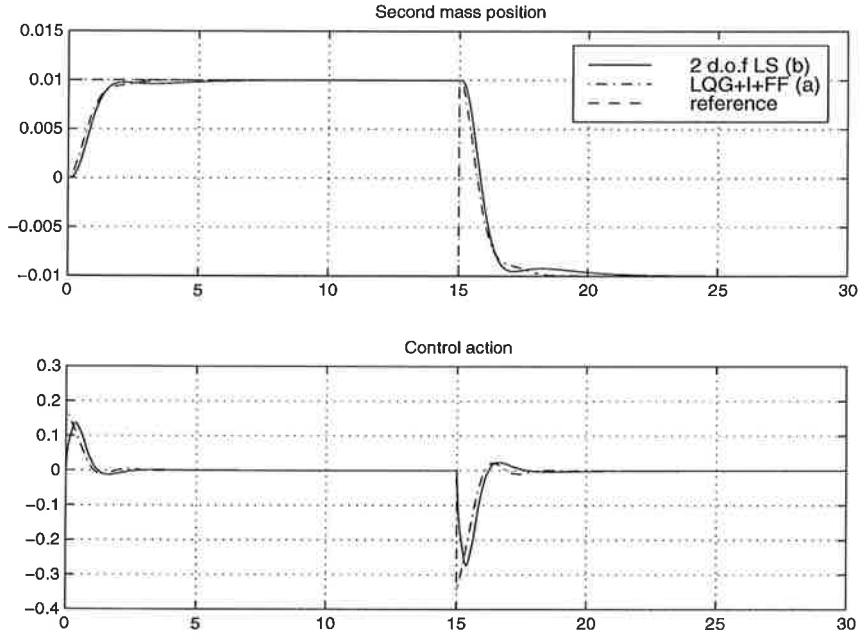

Figure 7.14: (3). Varying damping : c_2-3

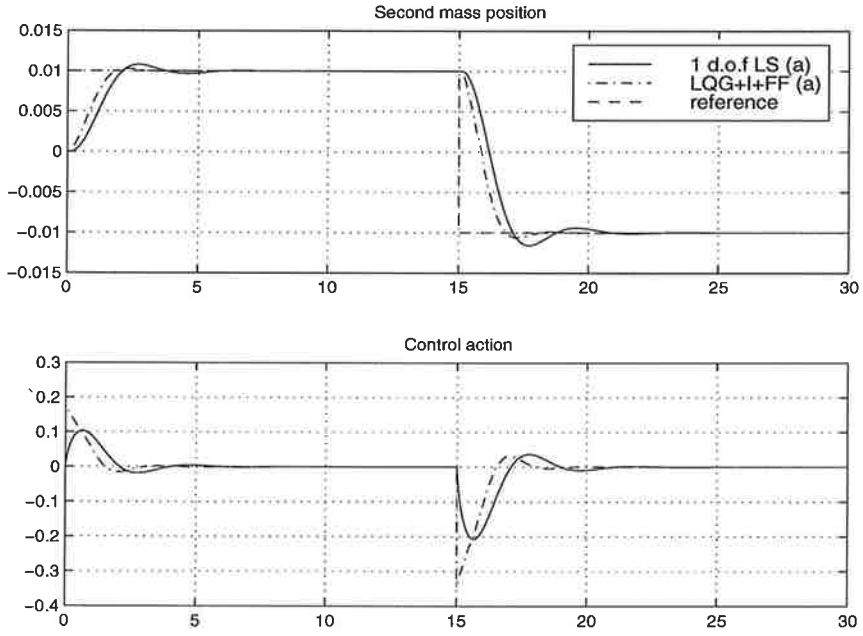

Figure 7.15: (3). Varying mass : m_2+1.5

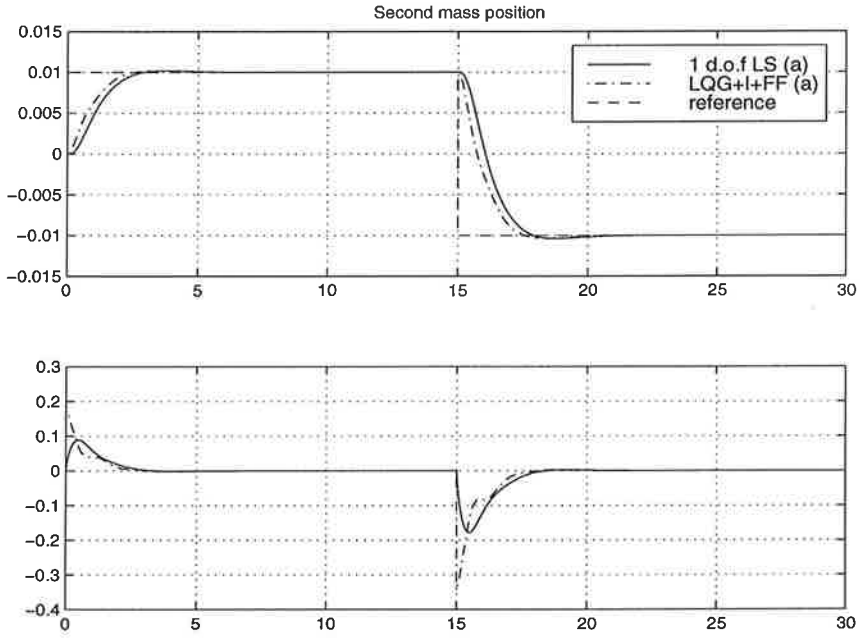

Figure 7.16: (3). Varying mass : m_2-1.5

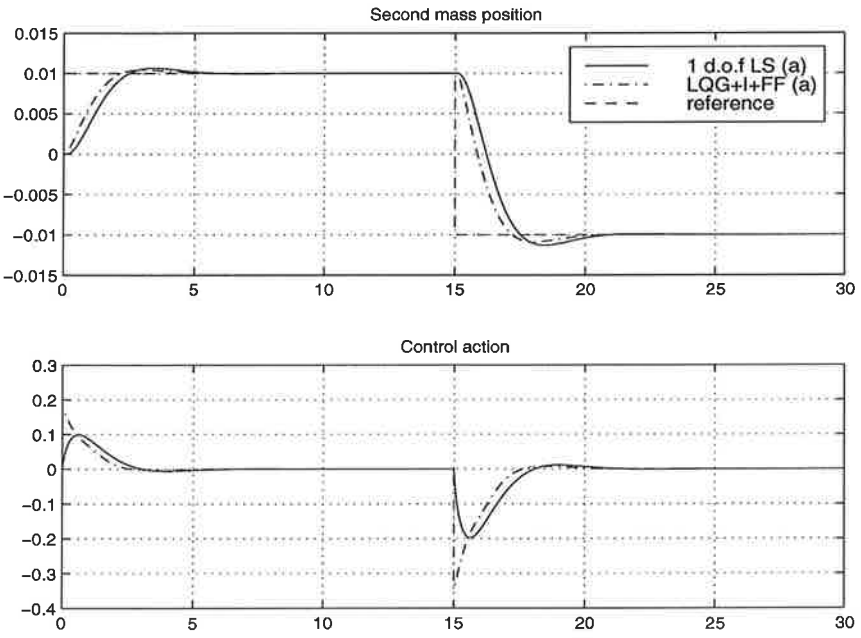

Figure 7.17: (3). Varying damping : c_2+3

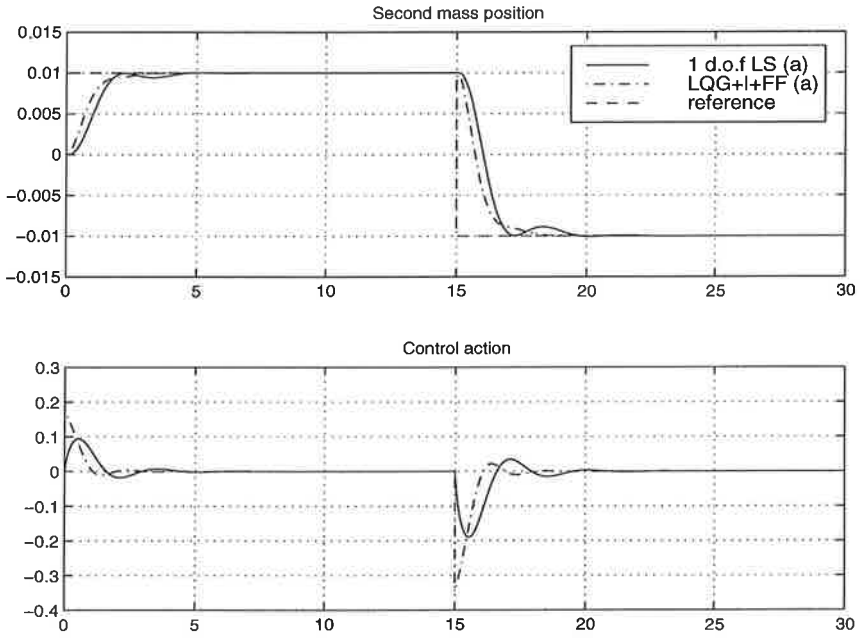

Figure 7.18: (3). Varying damping : c_2-3

7.1.4 Fourth group of controllers

The controllers to be compared in this subsection are the second "LQG+I+FF" with Q=750I, the 2 D.O.F loop-shaping controller designed with the low order weight (a) and the mixed sensitivity controller. The latter gives very good results in the simulations, but it doesn't have integral action so it is not useful for the real plant as it was explained in section 5.2. In figures 7.19 to 7.23 the "LQG+I+FF" is compared with the mixed sensitivity controller, and in figures 7.24 to 7.28 with the 2 D.O.F loop-shaping controller. In this last comparison we can see both controllers give similar results.

-	nominal	m_2+1.5	m_2-1.5	c_2+3	c_2-3
LQG+I+FF (b)	t_s=1.1 os=2	t_s=1.9 os=12	t_s=1.4 os=2	t_s=2.3 os=6	t_s=2.1 os=(0)
Mixed Sens.	t_s=1.1 os=0	t_s=2.0 os=6	t_s=1.8 os=0	t_s=2.0 os=0	t_s=1.9 os=13
2 d.o.f LS (a)	t_s=1.2 os=0	t_s=2.2 os=8	t_s=1.8 os=2	t_s=1.5 os=5	t_s=2.8 os=(4)

Table 7.5: Fourth group of controllers

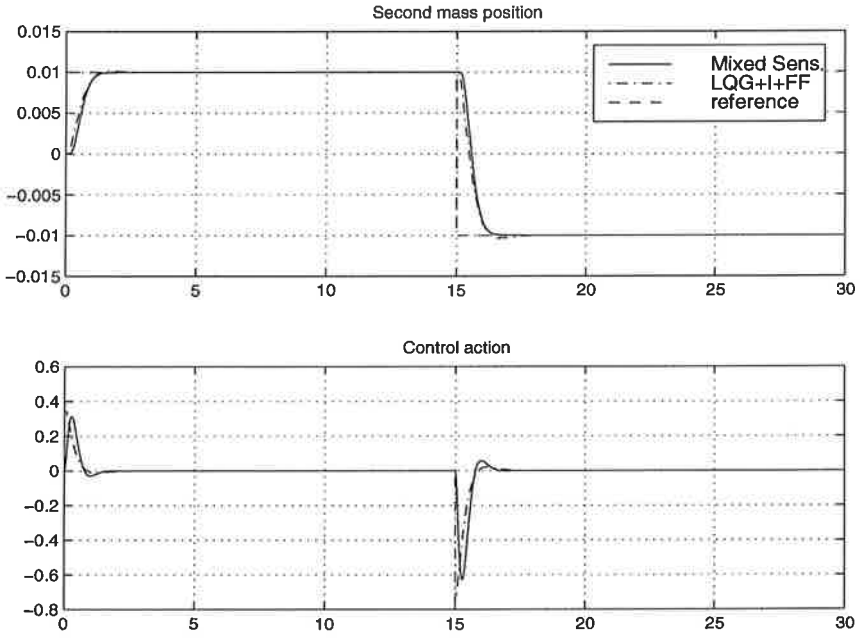

Figure 7.19: (4). Simulation with nominal plant

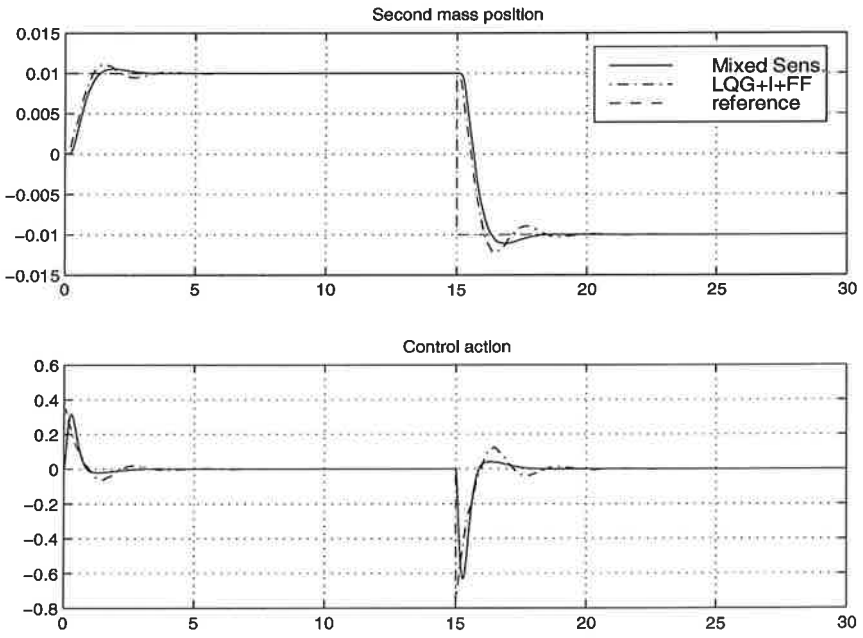

Figure 7.20: (4). Varying mass : m_2+1.5

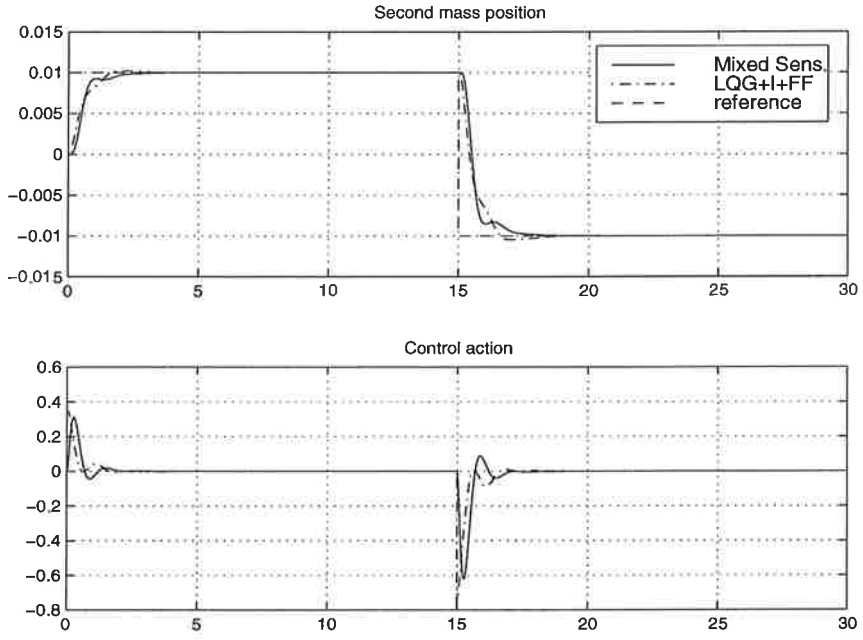

Figure 7.21: (4). Varying mass : m_2-1.5

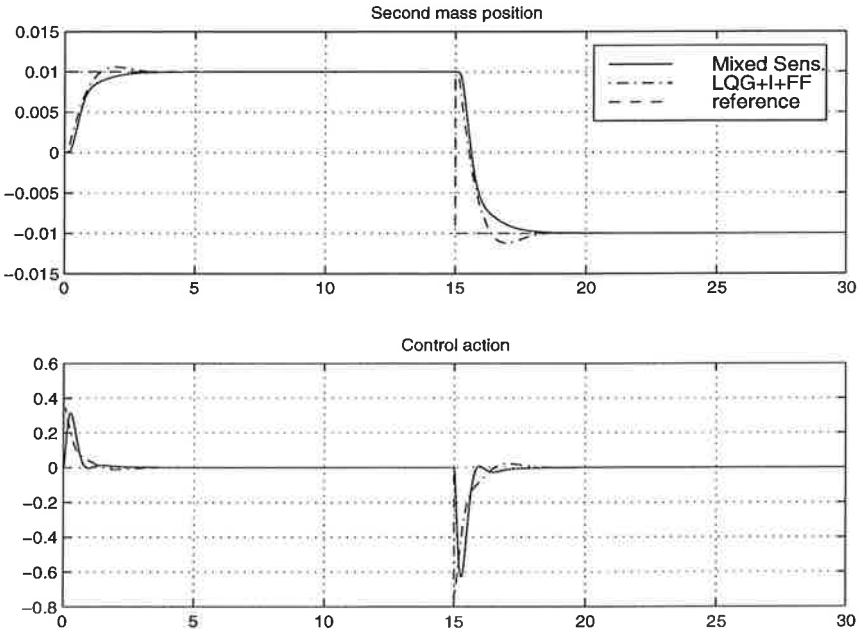

Figure 7.22: (4). Varying damping : c_2+3

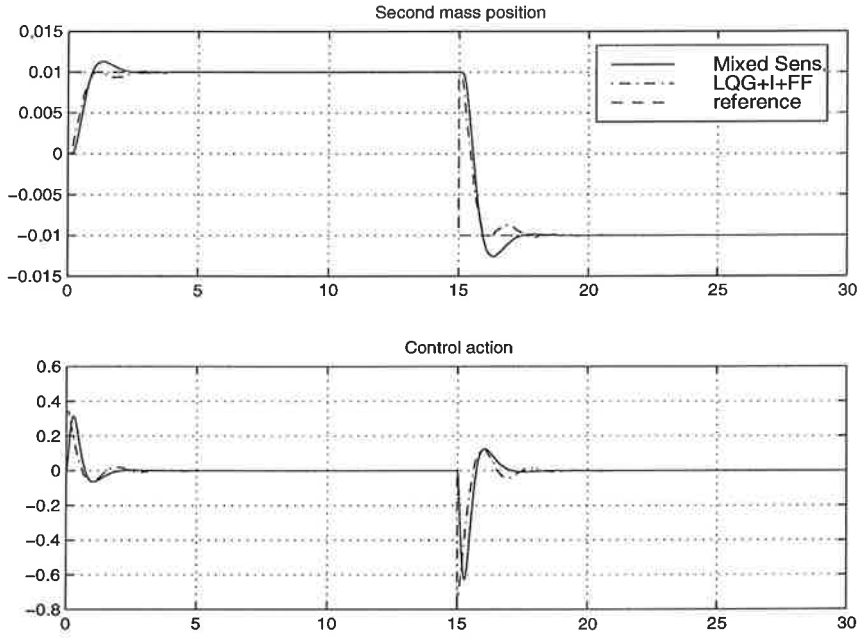

Figure 7.23: (4). Varying damping : c_2-3

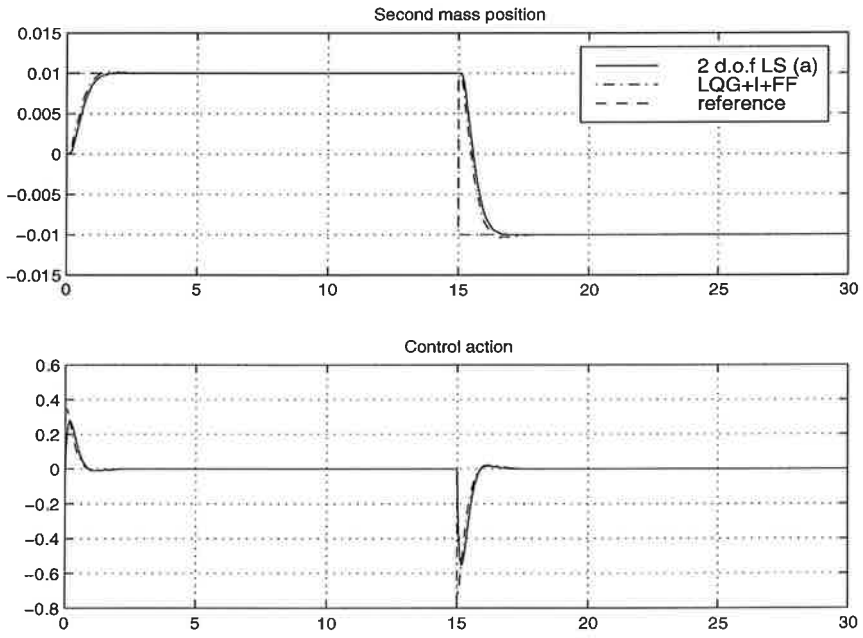

Figure 7.24: (4). Simulations with nominal plant

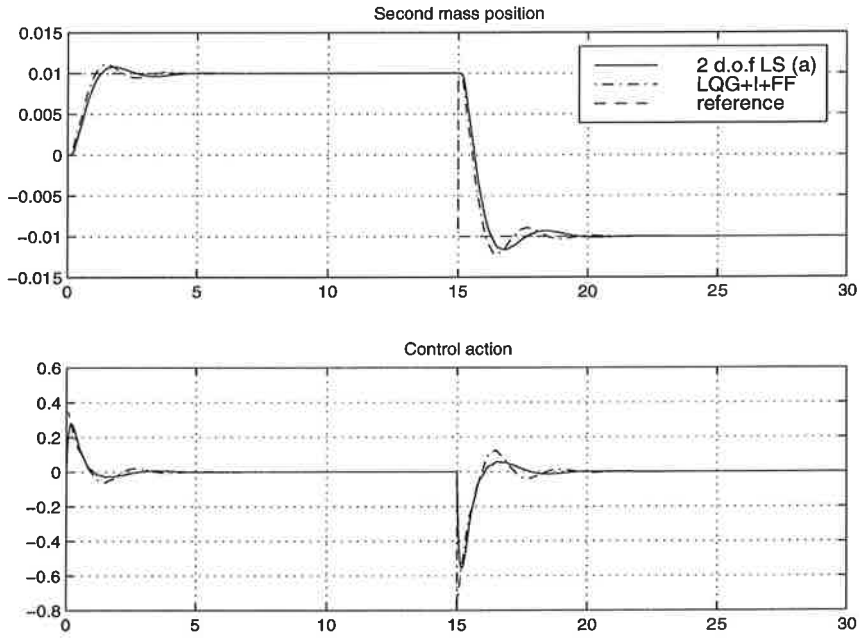

Figure 7.25: (4). Varying mass : m_2+1.5

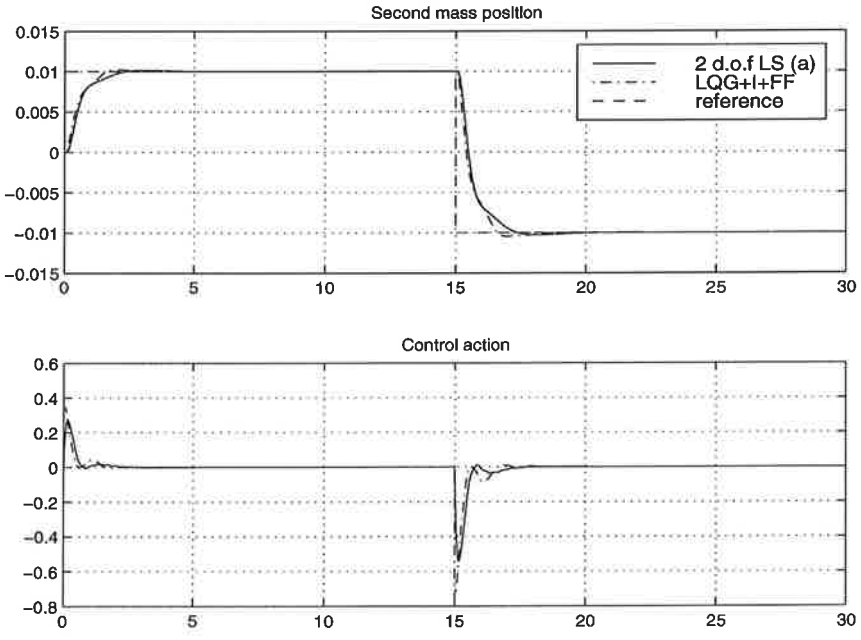

Figure 7.26: (4). Varying mass : m_2-1.5

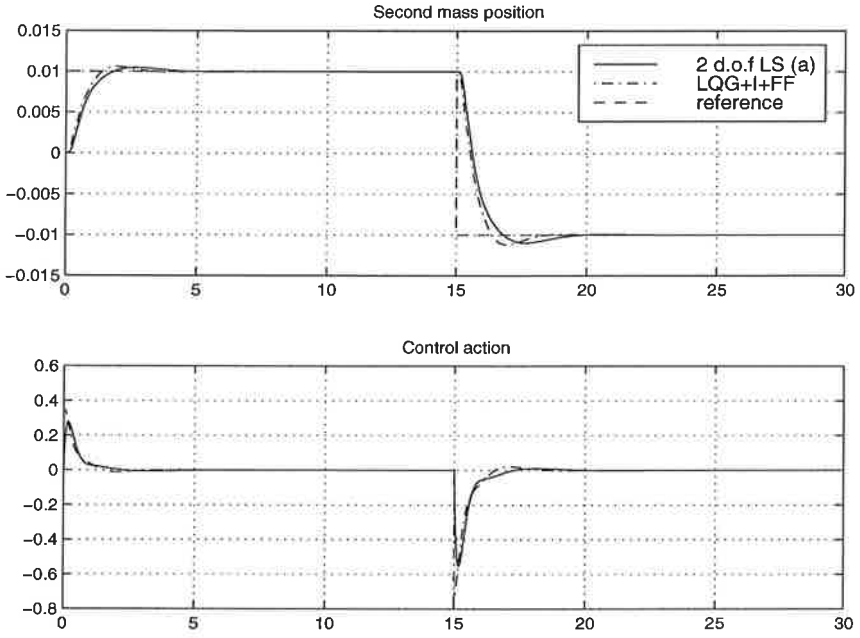

Figure 7.27: (4). Varying damping : c_2+3

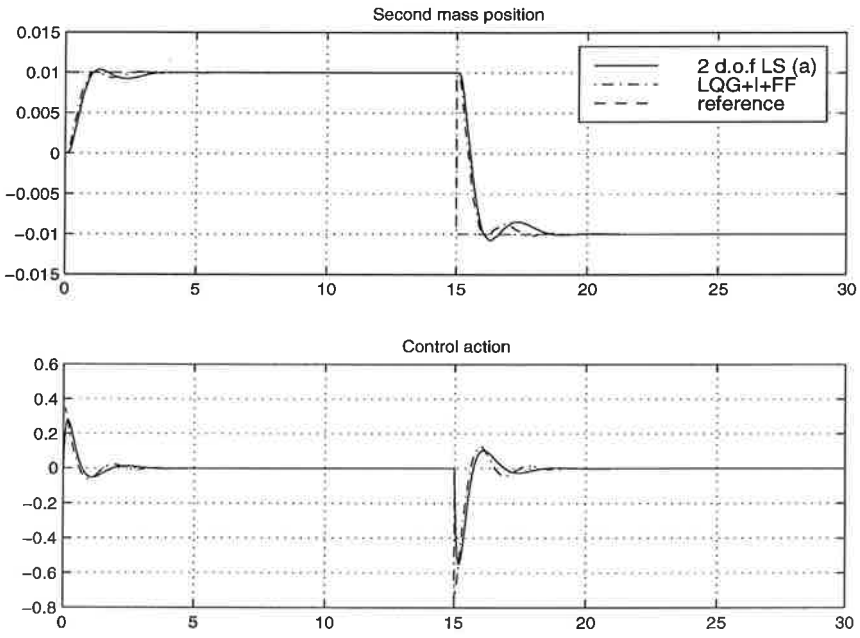

Figure 7.28: (4). Varying damping : c_2-3

7.2 Experiments

In this section, the tests with the experimental set up for the flexible servo are described. In all cases the plant parameter values are the nominal ones. Two controllers have been tried : the LQG+I+FF (b) and th 2 degrees-of-freedom loop-shaping controller (a). The reference input is not identical for all the tests, but we can consider they are qualitatively equivalent. They consist of a series of steps with different amplitudes and sign. The results of the tests are presented in figures 7.29 to 7.32. Looking at the graphs of the second mass position we can see that

- in some transients the mass sticks and slips giving the plot of the position the appearance of a "staircase".
- there are constant errors for long periods of time despite the presence of integral action in the controllers.
- there are "jumps" of the mass position.

These peculiarities are due to friction phenomena. When the masses draw close to the reference, they slow down. For low speeds friction may be bigger. In addition if the masses stop the control action must overcome the oposition of static friction which is always bigger than dynamic friction. Once there is enough energy to counteract this oposition, the masses may speed up too much producing the above mentioned "jumps". In industry this problem is sometimes called "hunting".

As for the control action, there is not a clear pattern. Working with the plant , one can notice it may be harder to move the masses in the positive direction than in the negative one. This may explain why most of the "jumps" occur for positive reference. Possible solutions may be

- to introduce a dead-zone before the integrator of the controller. With this solution there always will be steady-state error but we may avoid those "jumps".
- to get a better model of the process including all these friction phenomena and redesign the control.

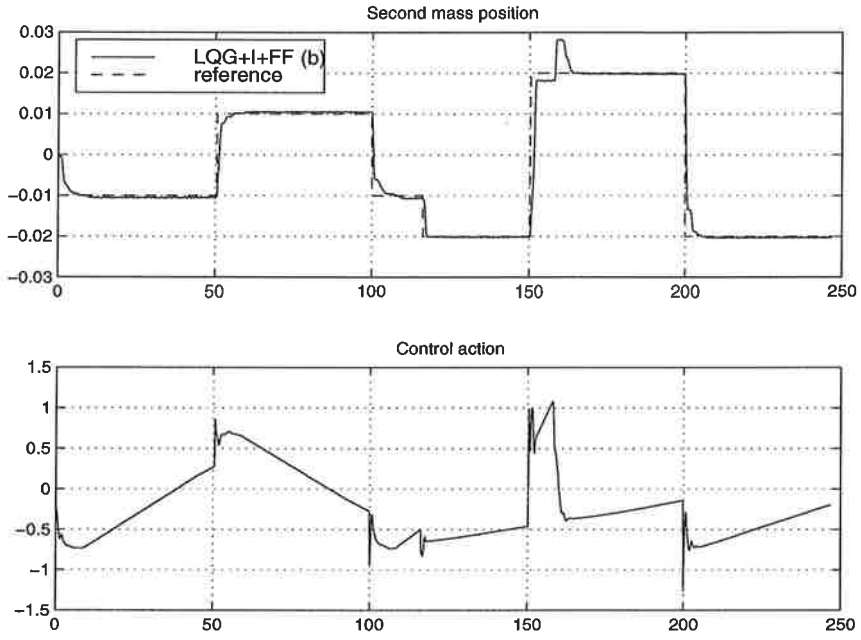

Figure 7.29: Test with LQG+I+FF (b)

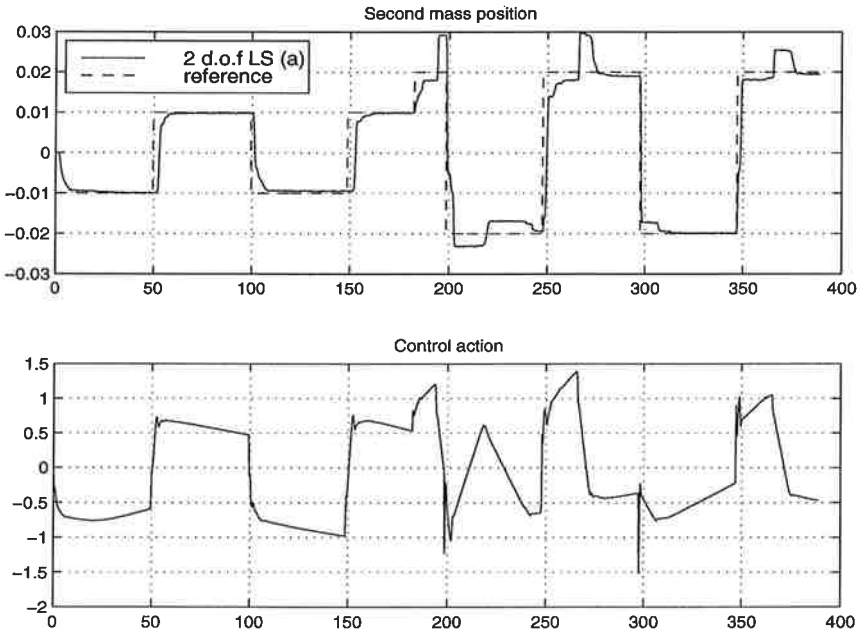

Figure 7.30: Test with 2 D.O.F Loop-shaping controller (a)

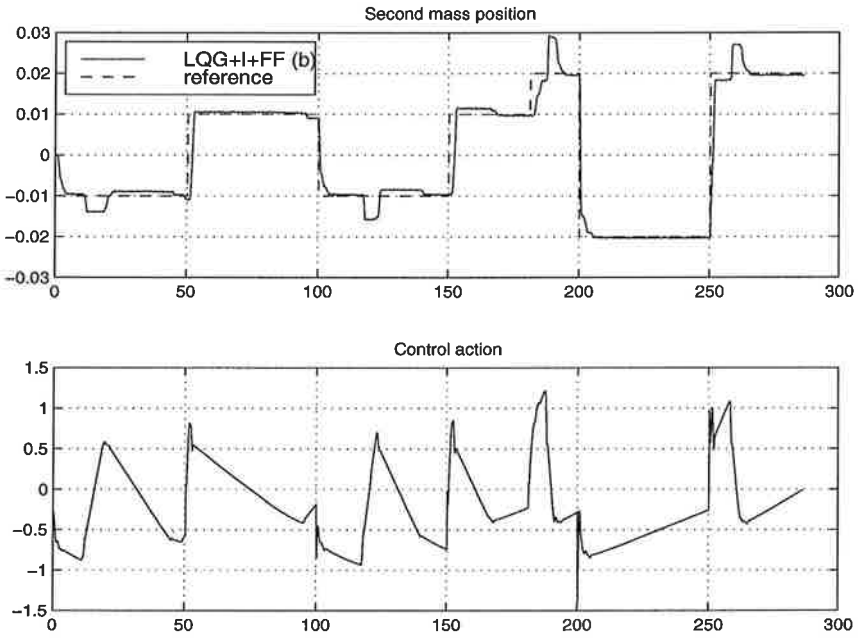

Figure 7.31: Test with LQG+I+FF (b)

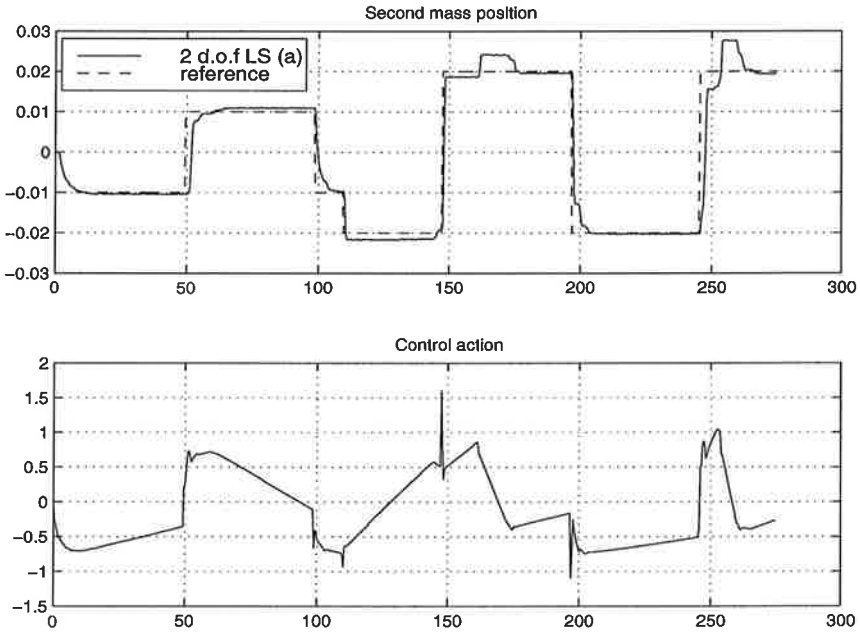

Figure 7.32: Test with 2 D.O.F Loop-shaping controller (a)

Chapter 8

Robust controller design based on linear programming

This chapter presents the calculations for a particular controller design problem to which the algorithm explained in [5] can be applied. Both unstructured and parametric uncertainty are dealt with, using the parametric coprime factor descriptions shown in section 3.2 . These plant descriptions are of the form

$$G_{\delta,\Delta} = \frac{\tilde{N}(s) + \delta\tilde{N}_\delta(s) + \Delta(s)\tilde{N}_\Delta(s)}{\tilde{M}(s) + \delta\tilde{M}_\delta(s) + \Delta(s)\tilde{M}_\Delta(s)} \tag{8.1}$$

where

- $\tilde{M}^{-1}\tilde{N}$ is the coprime factorization of a nominal transfer function. In our case this nominal transfer function corresponds, as in the previous $\mathcal{H}_\infty$ loop-shaping designs, to a weighted plant.
- $\tilde{M}_\delta$,$\tilde{M}_\Delta$,$\tilde{N}_\delta$, $\tilde{N}_\Delta$ are all fixed known transfer matrices with elements in $\mathbf{RH}_\infty$.
- $\delta \in \mathbf{R}^m$ and $\Delta \in \mathbf{RH}_\infty$ are uncertain but bounded in norm.

In our particular case we use the representation derived from the block diagram shown in figure 3.3. In that case

$$G_{\delta,\Delta} = \frac{\tilde{N}(s) + \delta\tilde{N}_\delta(s) + \Delta_N(s)}{\tilde{M}(s) + \delta\tilde{M}_\delta(s) + \Delta_M(s)} \tag{8.2}$$

and consequently, in the more general form $\Delta = [\Delta_N \quad \Delta_M]$ with $\tilde{N}_\Delta(s)^T = [1 \quad 0]$ and $\tilde{M}_\Delta(s)^T = [0 \quad 1]$.

Then, following [9] as explained in Appendix C, the condition used for controller design is

$$\begin{bmatrix} 1 + [\delta \quad \Delta] \begin{bmatrix} -\tilde{N}_\delta & \tilde{M}_\delta \\ -\tilde{N}_\Delta & \tilde{M}_\Delta \end{bmatrix} \begin{bmatrix} M & Y \\ N & X \end{bmatrix} \begin{bmatrix} Q \\ 1 \end{bmatrix} \end{bmatrix}^{-1} \in \mathbf{RH}_\infty \tag{8.3}$$

and the controller is

$$K = (Y - MQ)(X - NQ)^{-1} = (\tilde{X} - Q\tilde{N})^{-1}(\tilde{Y} - Q\tilde{M}) \quad Q \in \mathbf{RH}_\infty$$

As mentioned above, a shaped plant

$$G_s = GW_1$$

is used in order to "introduce" performance specifications.The weights used for the weighted plant are those already presented in chapter 6 :

$$W_1 = \frac{200(s + 2.656)}{s\,(s + 12.24)} \qquad \text{(a)}$$

and

$$W_1 = \frac{900(s + 1)^2}{s\,(s + 8)^2} \qquad \text{(b)}$$

In order to get $\tilde{N}$, $\tilde{M}$, N, X, Y, we can use the method shown in Appendix B. In the SISO case $\tilde{N} = N$, $\tilde{M} = M$, ... To get the other entries in (8.2) it is necessary to know first the transfer function of the perturbed plant with $[m_2\ ,\ c_2]$ as uncertain parameters

$$G_\delta = \frac{k}{(g_1 g_2 - k^2) + \delta_1 g_1 s^2 + \delta_2 g_1 s}$$

where $g_1 = m_1 s^2 + c_1 s + k$ and $g_2 = m_2 s^2 + c_2 s + k$. The perturbed plant when weighted becomes

$$G_{\delta s} = \frac{W_1 k}{(g_1 g_2 - k^2) + \delta_1 g_1 s^2 + \delta_2 g_1 s}$$

If for the nominal weighted plant

$$G_s = \tilde{M}^{-1}\tilde{N}$$

then we can define a factor $\frac{1}{\tilde{p}}$ such that

$$\frac{\tilde{N}}{W_1 k} = \frac{\tilde{M}}{(g_1 g_2 - k^2)} = \frac{1}{\tilde{p}}$$

and consequently it may be assumed that

$$\tilde{M}_\delta = \begin{bmatrix} \frac{g_1 s^2}{\tilde{p}} \\ \frac{g_1 s}{\tilde{p}} \end{bmatrix}$$

with $\delta = [\delta_1 \quad \delta_2]$. Since parameter k has been considered to be certain, $\tilde{N}_\delta = 0$. As for the unstructured uncertainty $\Delta = [\Delta_N \quad \Delta_M]$, it is possible to include the factor $\frac{1}{\tilde{p}}$ in a new unstructured Δ' where

$$\Delta'_N = \frac{\Delta_N}{\tilde{p}}$$

$$\Delta'_M = \frac{\Delta_M}{\tilde{p}}$$

Finally, we have $\tilde{N}_\Delta(s)^T = [1 \quad 0]$ and $\tilde{M}_\Delta(s)^T = [0 \quad 1]$.

Chapter 9

Conclusions

Within robust control there is a distinction between :

Robust stability The system is stable for all perturbed plants about the nominal model up to the worst-case model uncertainty.

Robust performance The system satisfies the performance specifications for all perturbed plants about the nominal model up to the worst-case model uncertainty.

In this thesis special attention has been payed to the second concept. Around it two parallel tasks have been developed. On one hand a series of control design techniques have been applied to an example of a flexible servo and finally compared. On the other hand two methods to represent parametric uncertainty have been analyzed, subject to a particular condition in order to be able to apply convex optimization. This analysis led to the choice of the second mass m_2 and damping c_2 as the only parameters to be regarded as uncertain. Turning back to the control techniques, these can be divided in two groups

- PI, PID and "LQG+I+FF" which have provided a reference for the performance to be expected from subsequent controllers.
- $\mathcal{H}_\infty$ techniques, specifically mixed sensitivity and $\mathcal{H}_\infty$ loop-shaping.

All controllers have been ranked according to their nominal performance. As the specifications become more demanding only the two degrees-of-freedom controllers are able to meet them. An exception is the mixed sensitivity design which nevertheless is not useful in practice, since the presence of a dead-zone in the plant makes necessary to have integral action in the controller. The two last two degrees-of-freedom controllers have been tried with the real plant. Their performance is very similar and in both cases the problems with friction are patent. A study of these problems and their possible

solutions could be an interesting topic for future work. Other interesting topic may be a more in-depth and analytical study of robustness.

Appendix A

Plant identification

Since the model of the plant is given, it is only necessary to identify the parameters. To do so a series of open loop experiments has been carried out. In order to get the parameters corresponding to one mass , the other one is blocked so the resulting system follows the differential equation

$$m\ddot{y} + c\dot{y} + ky = 0 \tag{A.1}$$

with characteristic equation

$$m\lambda^2 + c\lambda + k = 0 \tag{A.2}$$

$$\lambda = -\frac{c}{2m} \pm \sqrt{\frac{c^2}{4m^2} - \frac{k}{m}} \tag{A.3}$$

if $c^2 < 4mk$ then we have complex roots $-\alpha \pm i\beta$ where $\alpha = \frac{c}{2m}$ and $\beta = \sqrt{\frac{k}{m} - \frac{c^2}{4m^2}}$. The solution of the differential equation is of the form

$$y = A_1 e^{-\alpha t} \cos \beta t + A_2 e^{-\alpha t} \sin \beta t \tag{A.4}$$

or

$$y = A e^{-\alpha t} \sin(\beta t + \delta) \quad A, \delta \text{ const} \tag{A.5}$$

Equation (A.1) can be written as

$$\ddot{y} + 2\zeta\omega_n \dot{y} + \omega_n^2 y = 0 \tag{A.6}$$

so

$$\alpha = \zeta\omega_n \tag{A.7}$$

$$\beta = \omega_n \sqrt{1-\zeta^2} \tag{A.8}$$

In the experiments the mass is displaced a distance A from the origin and let free. So we have $\delta = 0$ and $t = \frac{2\pi n}{\beta}$. The initial position of the mass $y_0 = A$ and after n periods

$$y_n = Ae^{-\alpha t_n} = Ae^{-\frac{\alpha}{\beta}2\pi n} \tag{A.9}$$

with

$$\frac{\alpha}{\beta} = \frac{\zeta}{\sqrt{1-\zeta^2}} \tag{A.10}$$

Taking logarithm of y_n

$$\ln y_n = \ln A - \frac{\zeta}{\sqrt{1-\zeta^2}} 2\pi n \tag{A.11}$$

$$\frac{1}{2\pi n} \ln \frac{y_0}{y_n} = \frac{\zeta}{\sqrt{1-\zeta^2}} \tag{A.12}$$

With (A.8) and (A.12), and measuring experimentally y_0 , y_n and $\beta = \frac{2\pi n}{t_n - t_0}$, the parameters ζ and ω_n are calculated. Knowing each brass weight has a mass of $500 \pm 5g$ we can do several experiments with different number of masses in the carriage. Calling the combined mass of the weights in the carriage m_w, we can solve for the unloaded carriage mass m_c and spring constant k :

$$\begin{aligned} \frac{k}{m_w + m_c} &= \omega_{n1}^2 \\ \frac{k}{m_c} &= \omega_{n2}^2 \end{aligned} \tag{A.13}$$

The damping coefficient is found equating the first order terms in the equation forms

$$s^2 + 2\zeta\omega_n s + \omega_n^2 = s^2 + \frac{c}{m}s + \frac{k}{m} \tag{A.14}$$

The main results of the parameter identification are in section 2.1 "Description of the plant".

Appendix B

Coprime factor descriptions

In this appendix, the method to get the coprime factorizations of $G(s)$ is outlined. The main references are [4] and [8].

For each proper real-rational matrix G there exist eight $\mathbf{RH}_\infty$-matrices satisfying

$$G = NM^{-1} = \tilde{M}^{-1}\tilde{N}$$

which are the right and left-coprime factorizations of G, and

$$\begin{bmatrix} \tilde{X} & -\tilde{Y} \\ -\tilde{N} & \tilde{M} \end{bmatrix} \begin{bmatrix} M & Y \\ N & X \end{bmatrix} = I$$

The method starts with a minimal state-space realization of G, with [A,B,C,D] real matrices and (A,B) stabilizable, (C,A) detectable:

$$\begin{aligned} \dot{\boldsymbol{x}} &= A\boldsymbol{x} + B\boldsymbol{u} \\ \boldsymbol{y} &= C\boldsymbol{x} + D\boldsymbol{u} \end{aligned}$$

A real matrix F is chosen such that $A_F = A + BF$ is stable, and the vector $v = u - Fx$ and the matrix $C_F = C + DF$ are defined. Then

$$\begin{aligned} \dot{\boldsymbol{x}} &= A_F\boldsymbol{x} + B\boldsymbol{v} \\ \boldsymbol{u} &= F\boldsymbol{x} + \boldsymbol{v} \\ \boldsymbol{y} &= C_F\boldsymbol{x} + D\boldsymbol{v} \end{aligned}$$

The transfer matrix from v to u is

$$M(s) = I + F(s - A_F)^{-1}B$$

and that from v to y

$$N(s) = D + C_F(s - A_F)^{-1}B$$

therefore

$$u = Mv \ , \ y = Nv$$

so that $y = NM^{-1}u = Gu$.

Factors $\tilde{M}$ and $\tilde{N}$ are built similarly choosing a real matrix H such that $A_H = A + HC$ is stable and defining $B_H = B + HD$. The state-space representations of $\tilde{M}$ and $\tilde{N}$ are $[A_H, H, C, I]$ and $[A_H, B_H, C, D]$ respectively. Matrices F and H can be chosen placing the poles of A_F and A_H arbitrarily whithin the complex left-half plane, but can also be built solving the *Generalized Control Algebraic Riccati Equation* given by

$$(A - BS^{-1}D^*C)^*X + X(A - BS^{-1}D^*C) - XBS^{-1}B^*X + C^*R^{-1}C = 0$$

and the *Generalized Filtering Algebraic Riccati Equation* given by

$$(A - BS^{-1}D^*C)Z + Z(A - BS^{-1}D^*C)^* - ZC^*R^{-1}CZ + BS^{-1}B^* = 0$$

with $R = I + DD^*$ and $S = I + D^*D$.The , so called, *control gain* F and *filter gain* H are

$$F = -S^{-1}(D^*C + B^*X$$
$$H = -(BD^* + ZC^*)R^{-1}$$

Formulas for X,Y,$\tilde{X}$,$\tilde{Y}$ can be found in [4].

Appendix C

Youla parameterization

Many synthesis problems can be formulated in the following way: given G, design K so that the feedback system

- is internally stable.
- acquires some additional desired property, for example, robust stability.

A method to solve these problems is to parametrize all Ks for which (1) is true, and then to see if there exists a parameter for which (2) holds. In our case, as explained in [9], using the Youla parameterization of internally stabilizing controllers we may assume that the admissible transfer functions from ω to z in figure 3.1 are given on the form

$$T_1 + T_2 Q$$

where $T_1 \in \mathbf{RH}_\infty^{m\times 1}$ and $T_2 \in \mathbf{RH}_\infty^{m\times n}$ are fixed and Q is any transfer matrix in $\mathbf{RH}_\infty^{n\times 1}$. If the uncertainty loop $\omega = \delta z$ is closed,the system becomes robustly stable if and only if

$$[1 - \delta(T_1 + T_2 Q)]^{-1} \in \mathbf{RH}_\infty \quad \text{for } |\delta| \leq 1$$

If the parametric coprime factor description is used, the condition for robust stability can be rewritten as

$$\left[1 + [\delta \quad \Delta] \begin{bmatrix} -\tilde{N}_\delta & \tilde{M}_\delta \\ -\tilde{N}_\Delta & \tilde{M}_\Delta \end{bmatrix} \begin{bmatrix} M & Y \\ N & X \end{bmatrix} \begin{bmatrix} Q \\ 1 \end{bmatrix}\right]^{-1} \in \mathbf{RH}_\infty$$

Robust performance problems can be rewritten as robust stability problems in a standard way, but the approach in [9] will apply only if they

have the form of an $\mathbf{H}_\infty$ bound on the response to a disturbance that enters additively to the signal ω.

A brief account of the Youla parameterization is given in the following lines. First it is useful to look at the standard set-up shown in figure C.1.

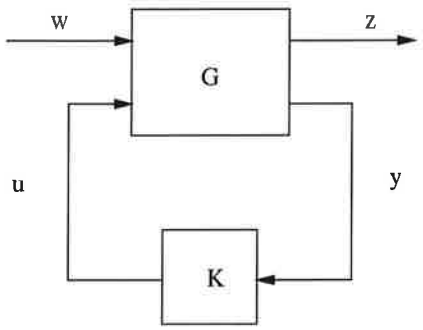

Figure C.1: Standard block diagram

In this figure ω is the exogenous input, tipically consisting of command signals, disturbances, and sensor noises;u is the control signal; z is the output to be controlled,tipically consisting of tracking errors, filtered actuator signals,etc.;y is the measured output. G represents a generalized plant that can be partitioned as

$$G = \begin{bmatrix} G_{11} & G_{12} \\ G_{21} & G_{22} \end{bmatrix}$$

so we have the algebraic equations

$$\begin{aligned} z &= G_{11}\omega + G_{12}u \\ y &= G_{21}\omega + G_{22}u \\ u &= Ky \end{aligned}$$

To define internal stability two additional inputs are introduced as in figure C.2.

If the nine transfer matrices from ω,ν_1,ν_2 to z,u,y are stable, then we say K stabilizes G. (To simplify the theory is usually assumed G_{22} is strictly proper so the nine transfer matrices mentioned above are proper).
In [4] it is proved that K stabilizes G if and only if K stabilizes G_{22}. To get a parameterization of all Ks which stabilize G_{22}, first a doubly-coprime factorization of G_{22} is obtained and then

$$K = (Y - MQ)(X - NQ)^{-1} = (\tilde{X} - Q\tilde{N})^{-1}(\tilde{Y} - Q\tilde{M}) \quad Q \in \mathbf{RH}_\infty$$

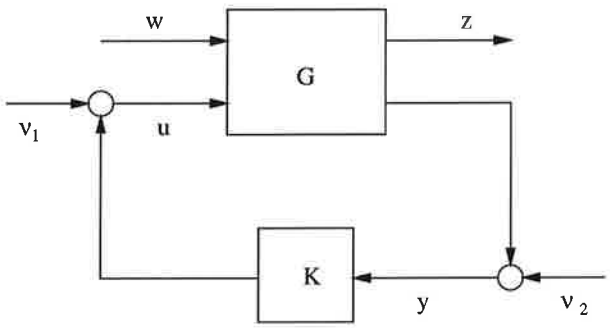

Figure C.2: Diagram for stability definition

Bibliography

[1] Åström,K.J., Wittenmark,B. (1996). *Computer Controlled Systems*, Prentice-Hall.

[2] Danielsson, Mikael.*Control of an oscillatory system.* Master thesis. ISRN LUTFD2/TFRT–5575–SE, Department of Automatic Control, Lund Institute of Technology, Lund, Sweden, March 1997.

[3] Doyle,J.C., Francis, B.A. and Tannenbaum,A.R. (1992). *Feedback Control Theory*,Macmillan Publishing Company.

[4] Francis,B.(1987).*A course in $\mathcal{H}_\infty$ control theory*,Lecture Notes in Control and Information Sciences, Springer-Verlag, Berlin.

[5] Ghulchak,A.,Rantzer,A.(1999)*Robust Controller Design Based on Linear Programming.* Submitted to CDC'99.

[6] Kwakernaak,H.(1993).*Robust Control and $\mathcal{H}_\infty$-Optimization - Tutorial Paper*, Automatica 29:255-273.

[7] Kwakernaak,H.(1995) *Symmetries in Control System Design*, in *Trends in Control: A European Perspective*, Alberto Isidori (Ed.), Springer-Verlag,Berlin.

[8] McFarlane,D.C.,Glover,K.(1990)*Robust Controller Design Using Normalized Coprime Factor Plant Descriptions*,,Lecture Notes in Control and Information Sciences, Springer-Verlag, Berlin.

[9] Rantzer,A.,Megretski,A.(1994).*A Convex Parameterization of Robustly Stabilizing Controllers*, IEEE Transactions on Automatic Control,39.

[10] Skogestad,S.,Postlethwaite,I.(1996).*Multivariable Feedback Control. Analysis and Design.*,Wiley.

[11] *Manual for Model 210/219a. Rectilinear Dynamic System.*(1996)ECP Educational Control Products.